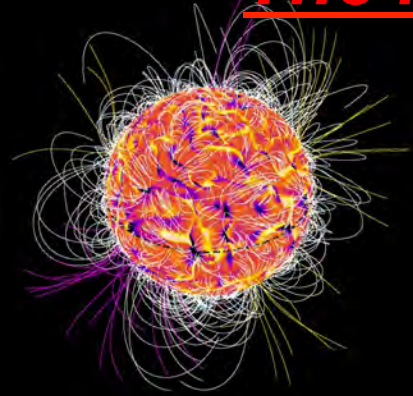
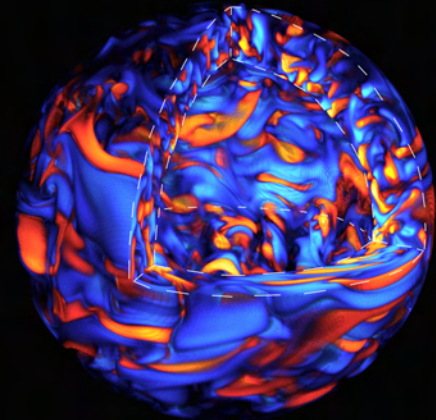


The New Concept of Stellar Spot Dynamo



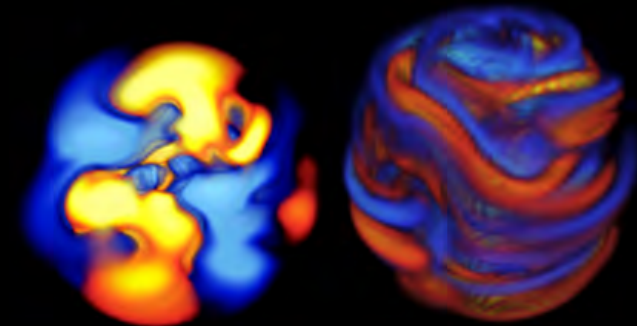
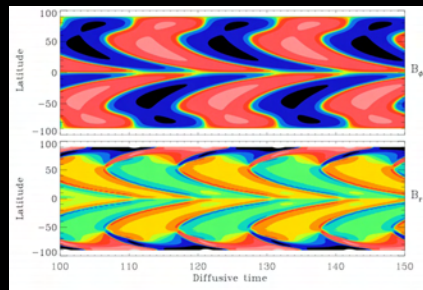
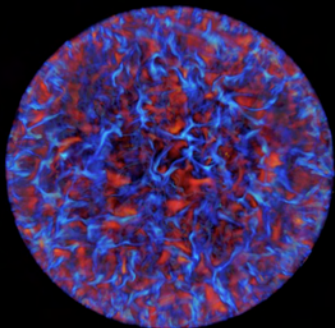
Allan Sacha Brun

Service d'Astrophysique/UMR AIM,
CEA-Saclay



with J. Toomre, M.S. Miesch, B. Brown, M. Browning,
L. Jouve, K. Augustson, A. Strugarek, C. Emeriau and the STARS2 Team

- Observational evidence of stellar rotation/magnetism
- 3-D simulations of solar-like stars

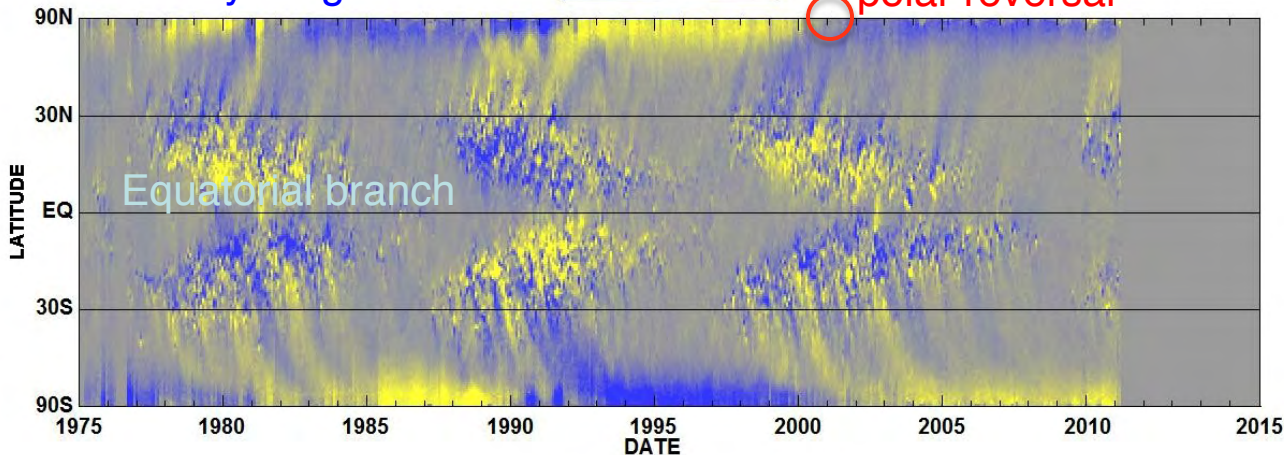


Solar Cycle and Rotation

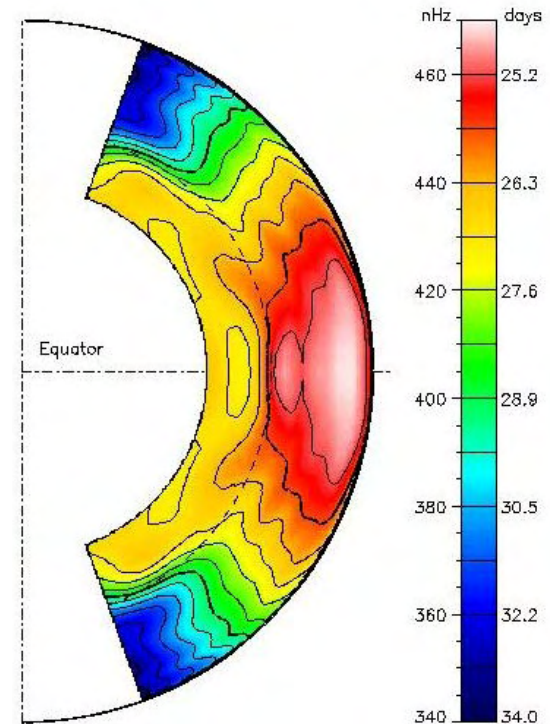
Butterfly Diagram

-10G -5G 0G +5G +10G

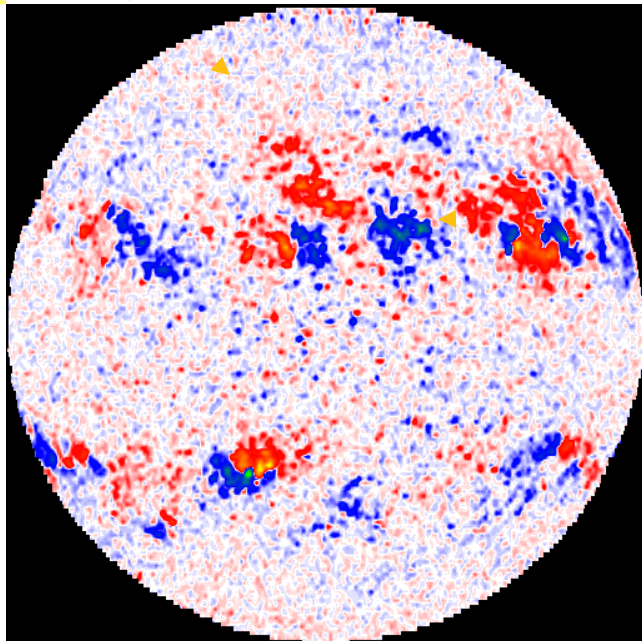
polar reversal



Hathaway/NASA/MSFC 2011/04

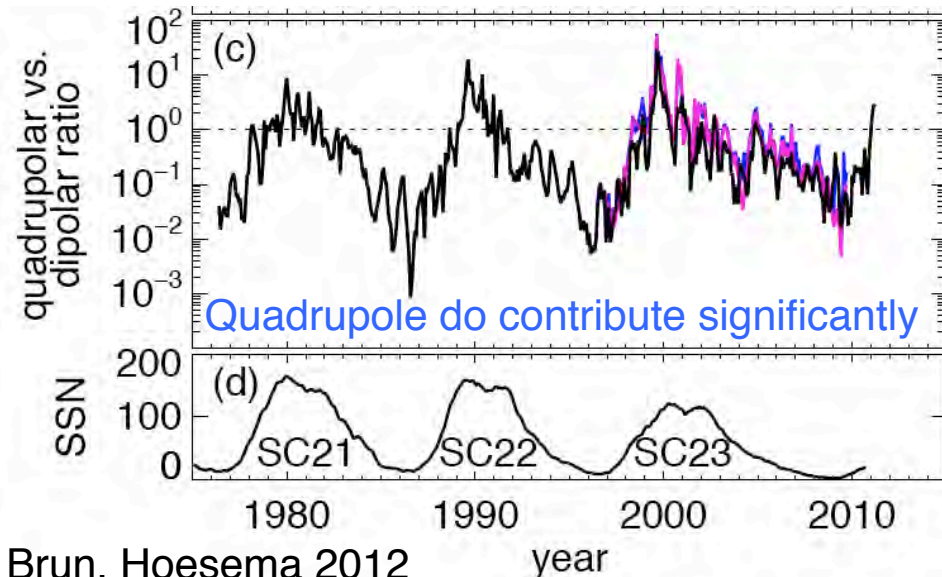


Quiet



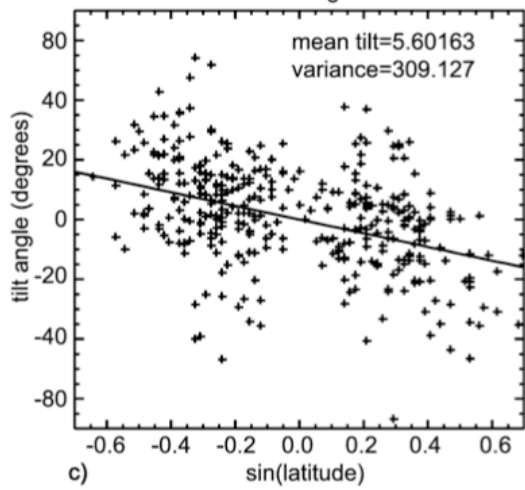
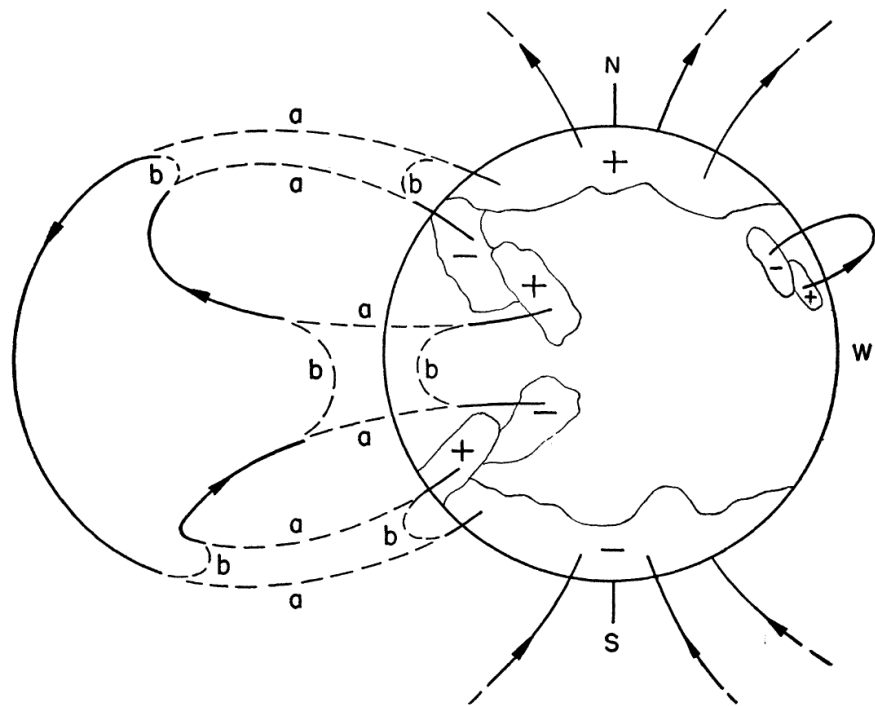
Small vs Large Scale Dynamos

Active



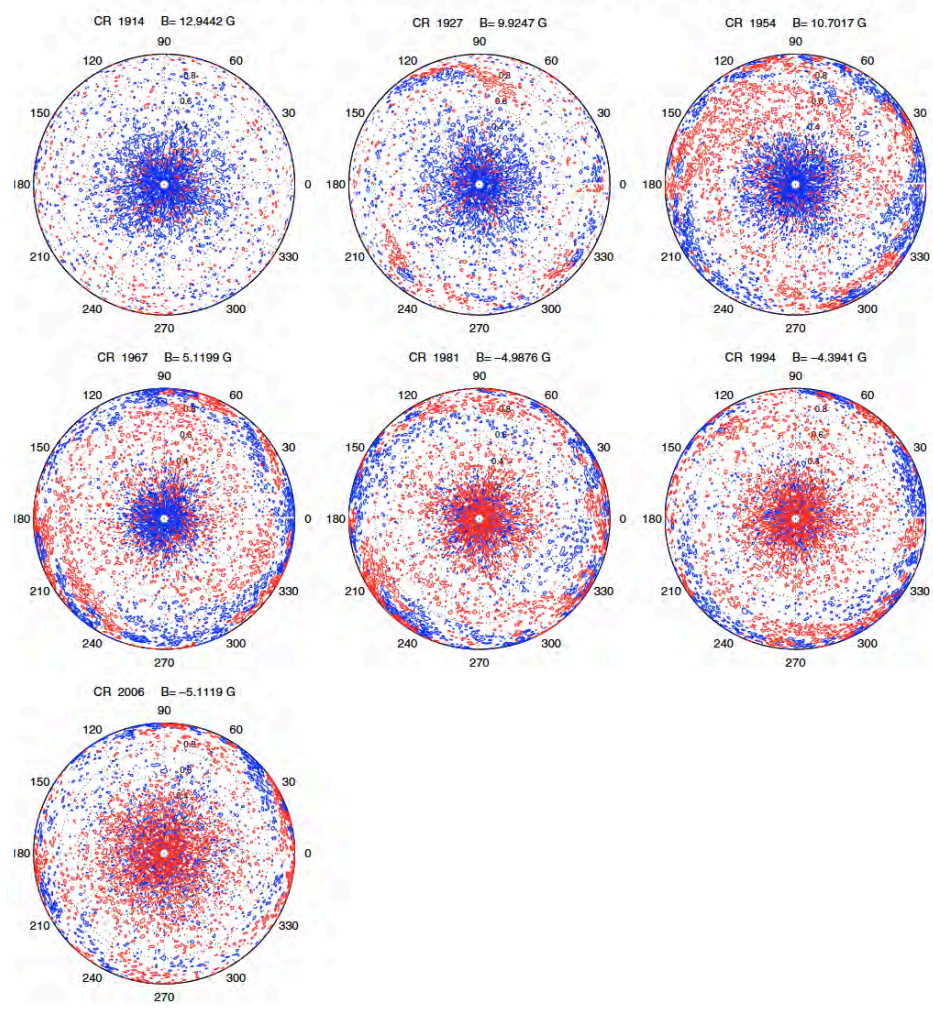
Derosa, Brun, Hoesema 2012

Babcock-Leighton Mechanism and Polar Cap Reversal



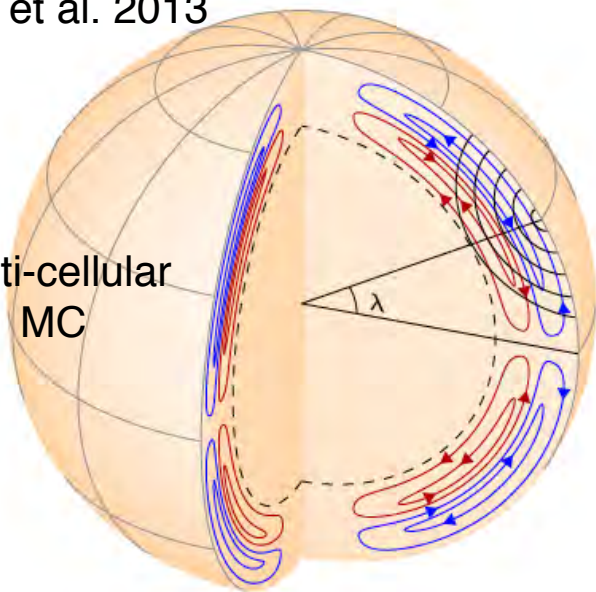
Joy's Law
Tilt of AR

E. E. Benevolenskaya: Polar magnetic flux on the Sun in 1996–2003 from SOHO/MDI data



How important
is it to get the 11yr
dynamo?

Multi-cellular
MC

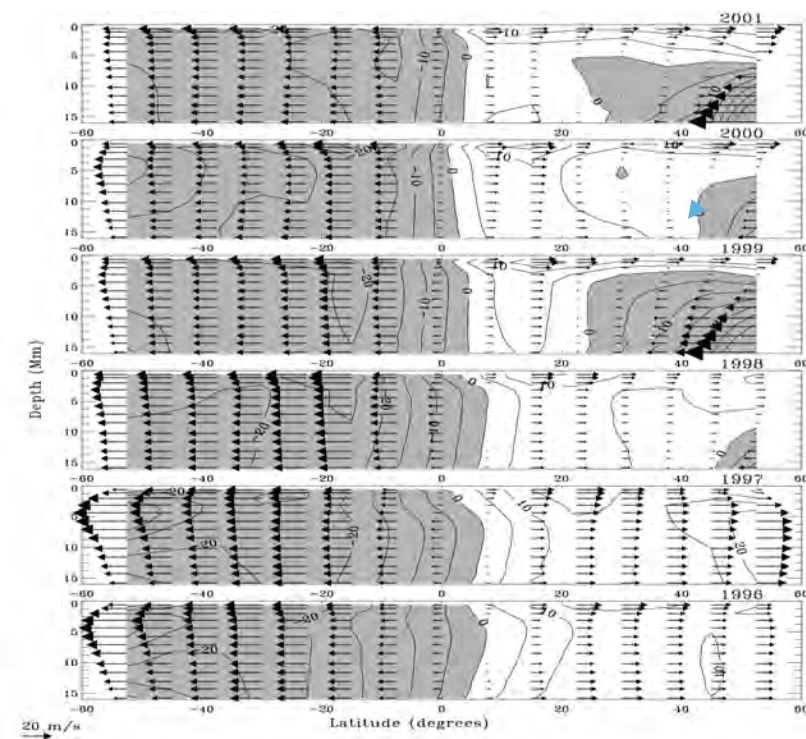
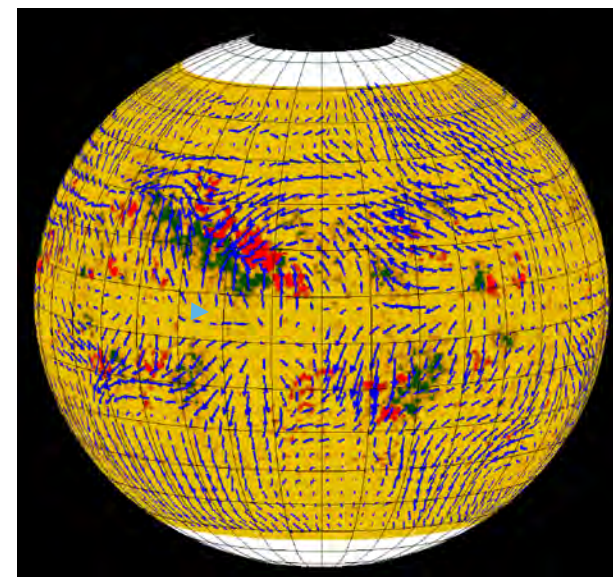


Meridional Circulation

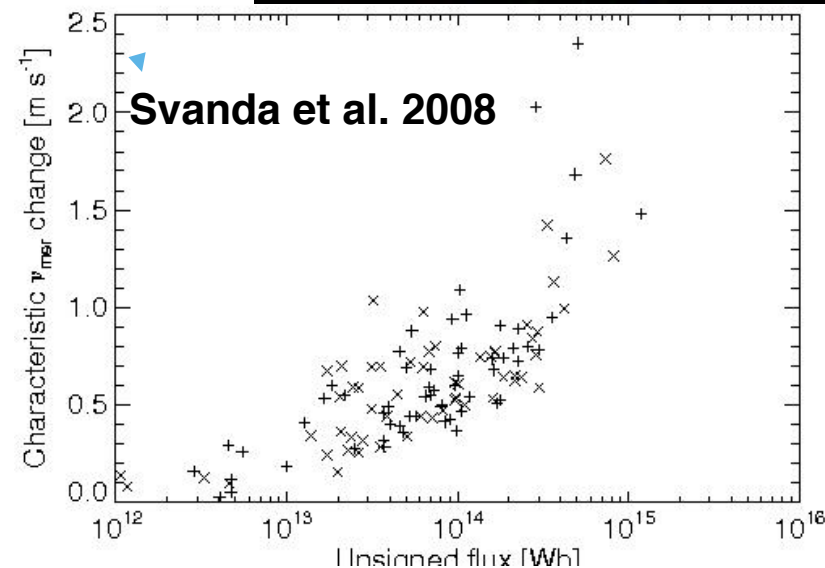
More & more evidence for multi cellular MC

Influence of B
(active region)
on MC

...



(Haber et al. 2002)

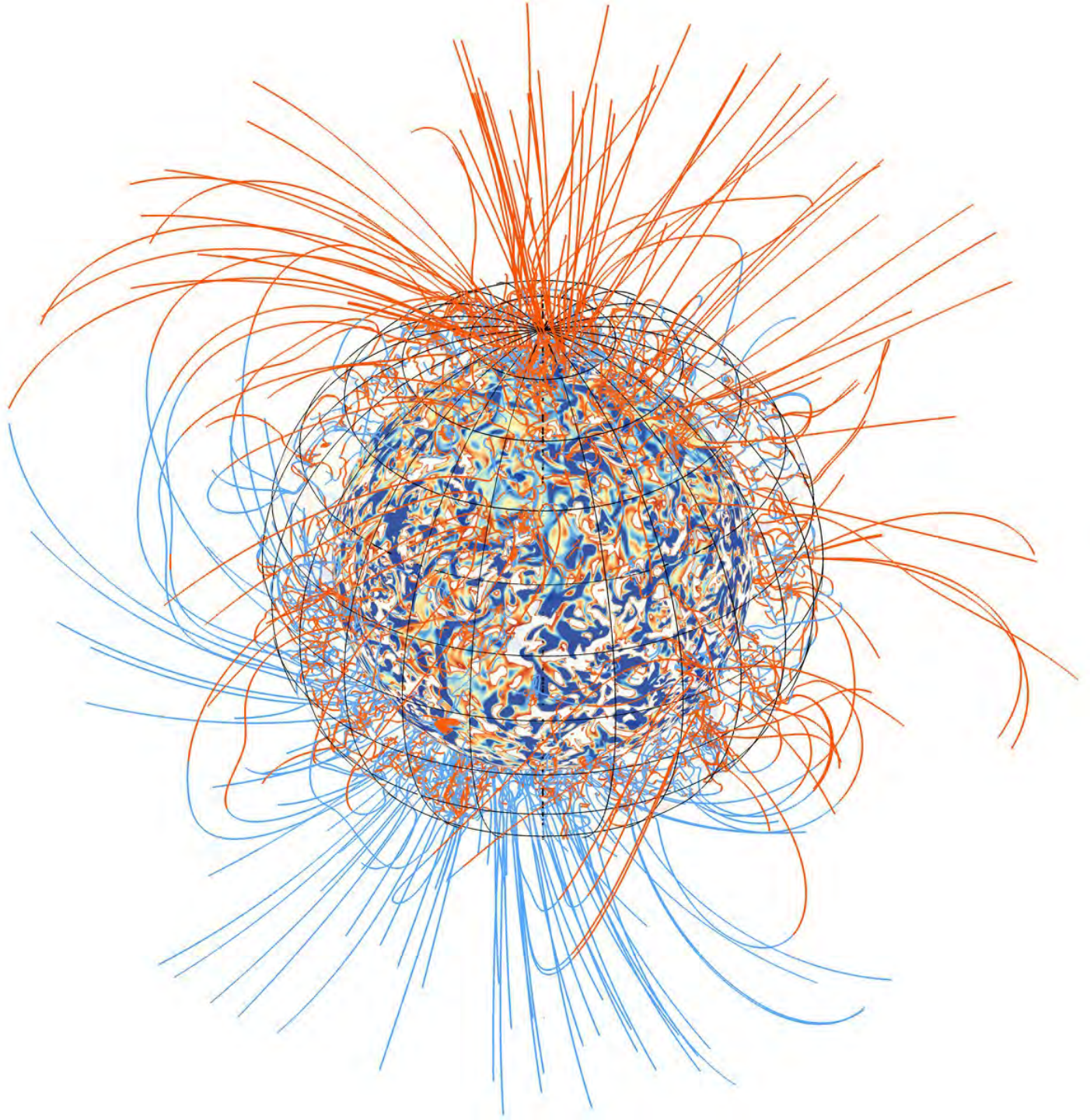


Svanda et al. 2008

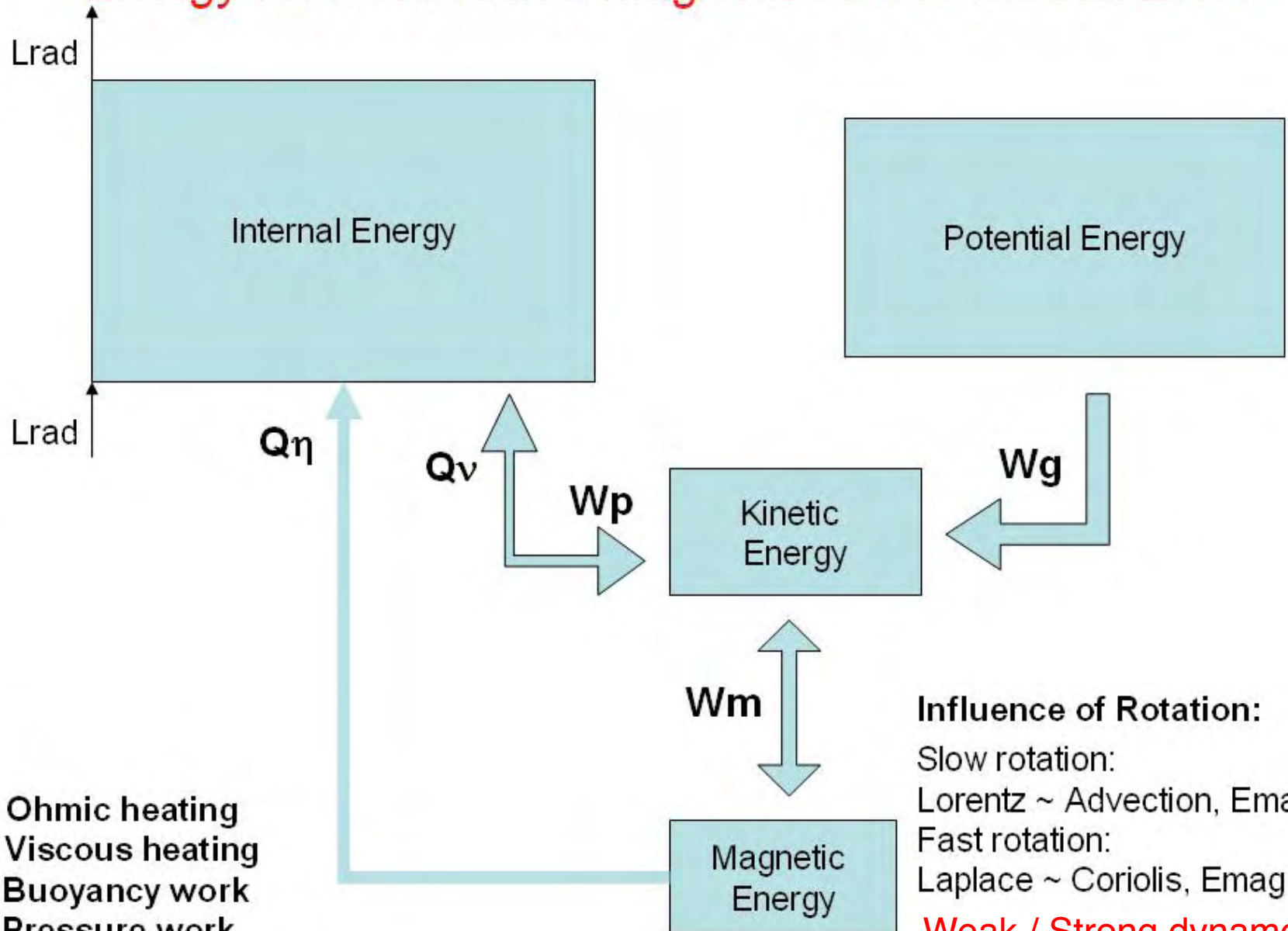
See also Hathaway et al. 1996, Gizon 2004, Zhao & Kosovichev 2004, etc...

Going 3-D: nonlinear convection dynamo MHD simulations

Magnetic field in a solar-like star dynamo



Energy Reservoirs in a Magnetized Convection Zone



Q_η : Ohmic heating
 Q_v : Viscous heating
 W_g : Buoyancy work
 W_p : Pressure work
 W_m : Lorentz force work

Influence of Rotation:

Slow rotation:
Lorentz \sim Advection, $E_{\text{mag}} \sim E_{\text{ke}}$
Fast rotation:
Laplace \sim Coriolis, $E_{\text{mag}} > E_{\text{ke}}$

Weak / Strong dynamo regime

Various Dynamo Regimes and Scalings

Equilibrium field : $B_{\text{eq}} \sim \sqrt{8\pi P_{\text{gaz}}} \sim \sqrt{\rho_*}$

If magnetic Reynolds number $Rm \sim 1$, $\nu = \eta/L$, then

Laminar (weak) scaling: Lorentz \sim diffusion \Rightarrow

$$B_{\text{weak}}^2 \sim \rho \nu \eta / L^2$$

Turbulent (equipartition) scaling: Lorentz \sim advection \Rightarrow

$$B_{\text{turb}}^2 \sim \rho v^2 \sim \rho \eta^2 / L^2 \Leftrightarrow |B_{\text{weak}}| \sim |B_{\text{turb}}| P_m^{1/2}$$

Magnetostrophic (strong) scaling: Lorentz \sim Coriolis \Rightarrow

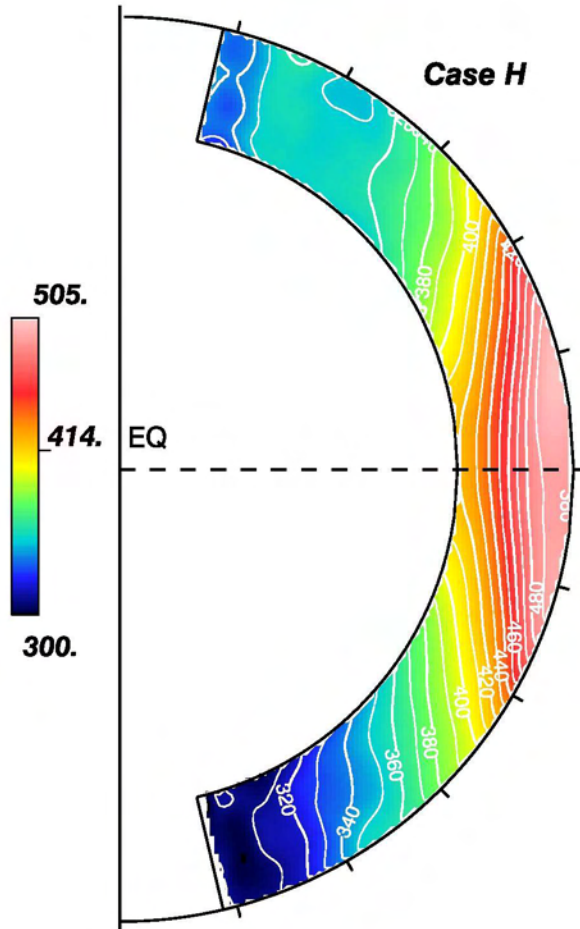
$$B_{\text{strong}}^2 \sim \rho \Omega \eta$$

With ρ density, ν kinematic viscosity, η magnetic diffusivity, Ω rotation rate, v , L characteristic velocity & length scales, $P_m = \nu/\eta$ the magnetic Prandtl nb

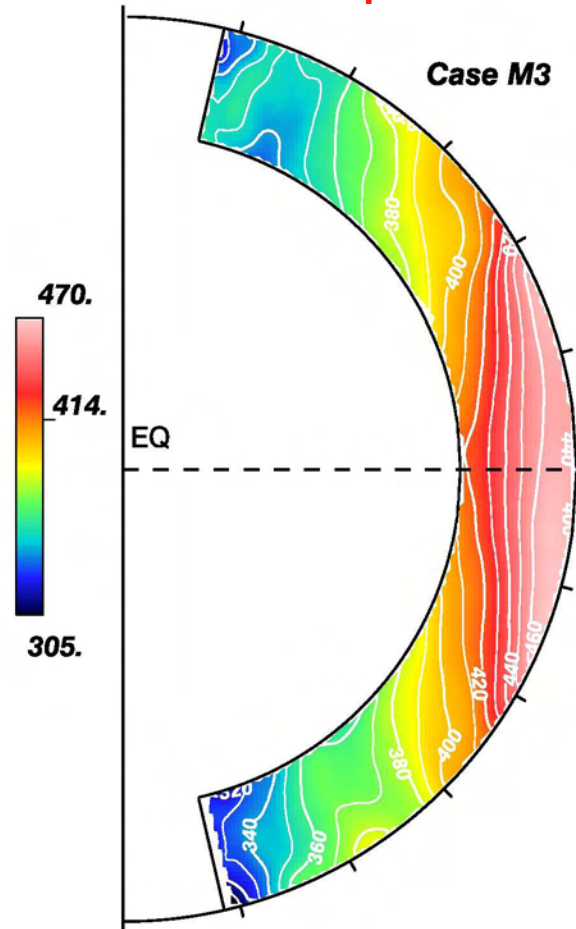
Fauve et al. 2010, Christensen 2010, Brun et al. 2013

Mean Angular Velocity Ω

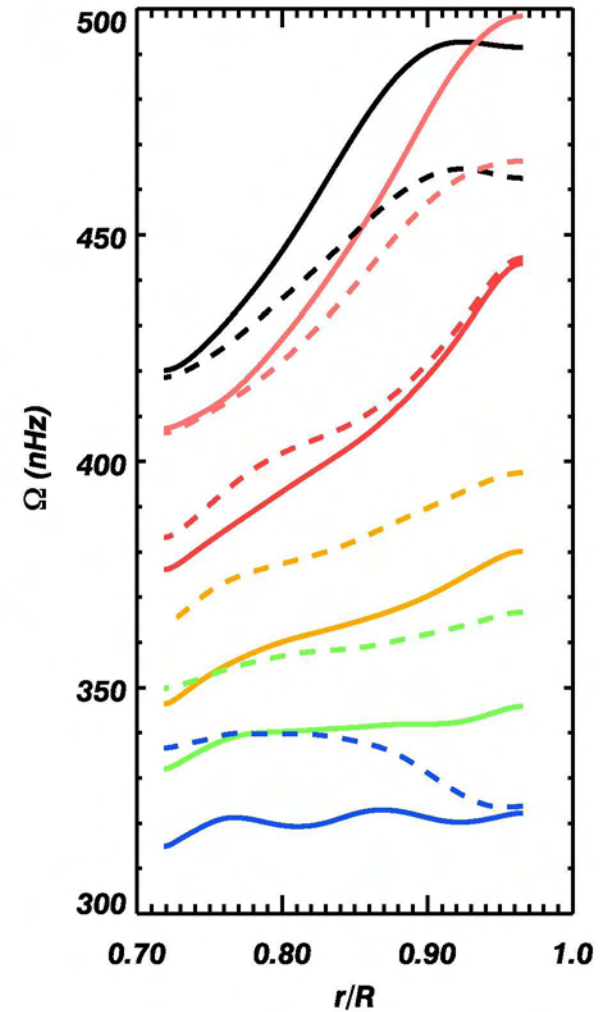
Ω quenching!



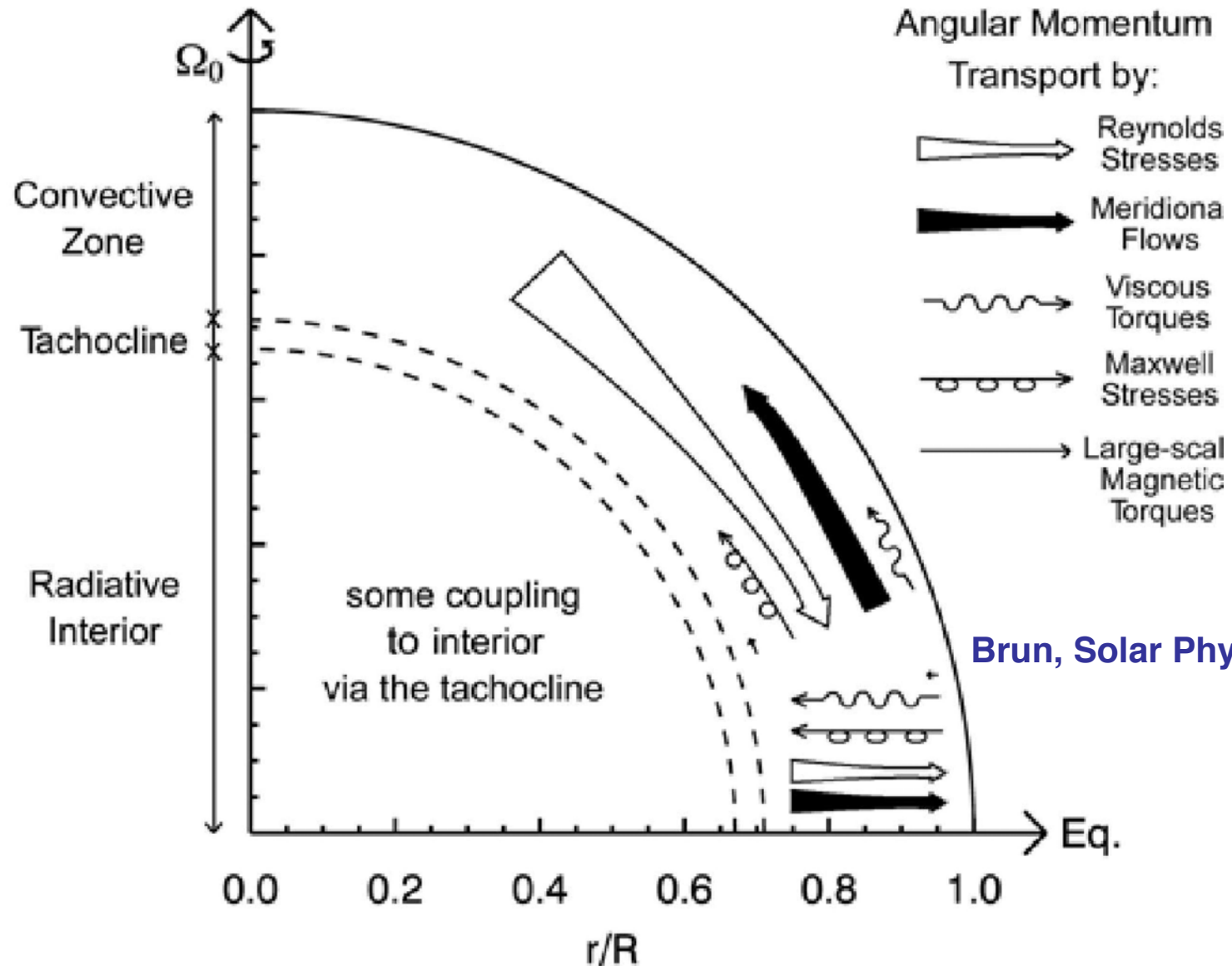
Initial state of differential rotation



Evolved state of differential rotation under
the influence of the **Lorentz force**



Angular Momentum Balance in Presence of B

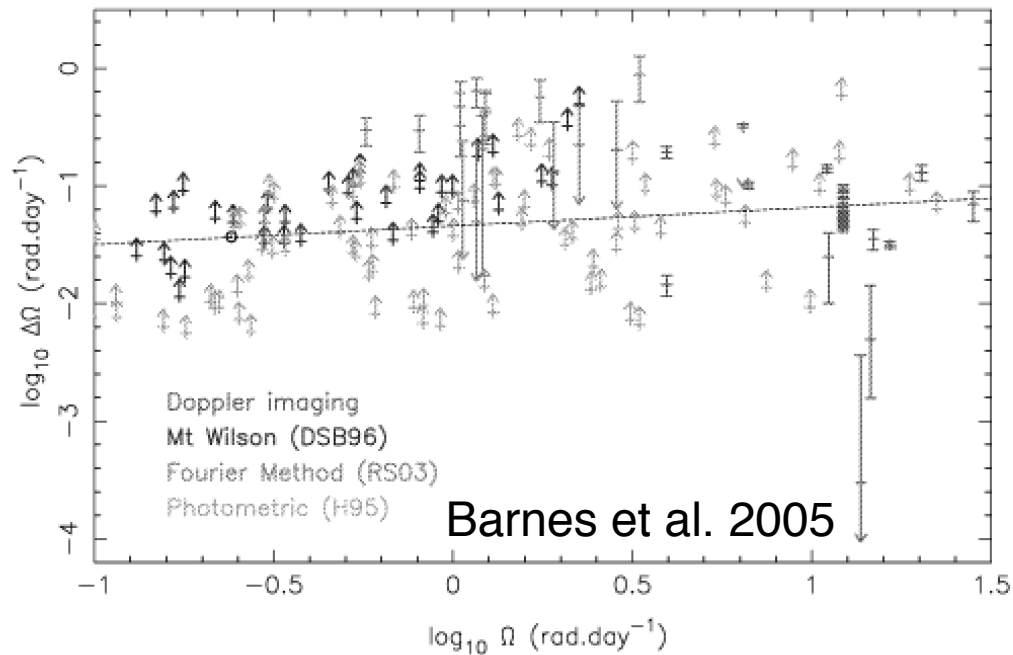


Brun, Solar Physics, 2004

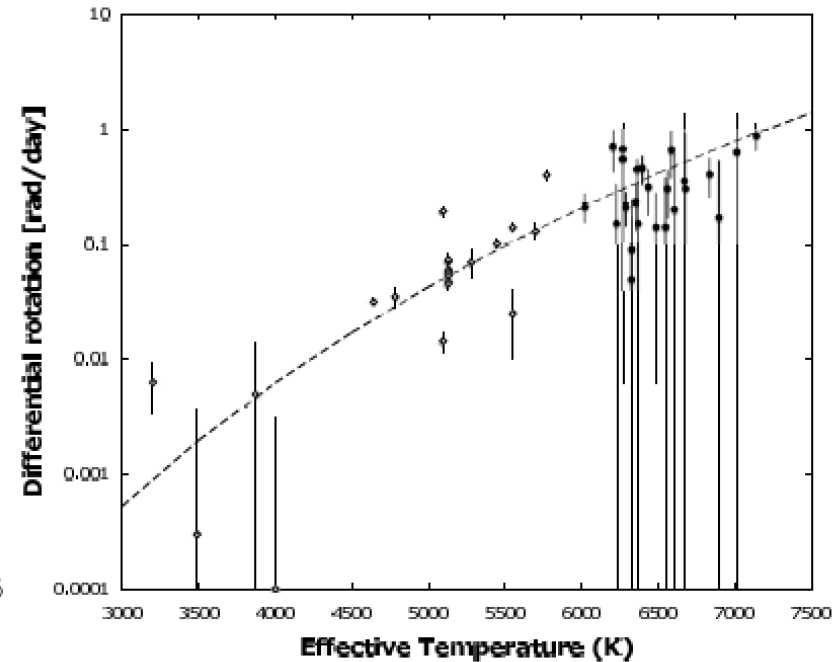
The transport of angular momentum by the **Reynolds stresses** remains at the **origin of the equatorial acceleration**. The **Maxwell stresses** seeks to speed up the poles.

Trends in Differential Rotation with Ω & Mass (Teff)

Weak trend with Ω



$\Delta\Omega$ increases with M_*



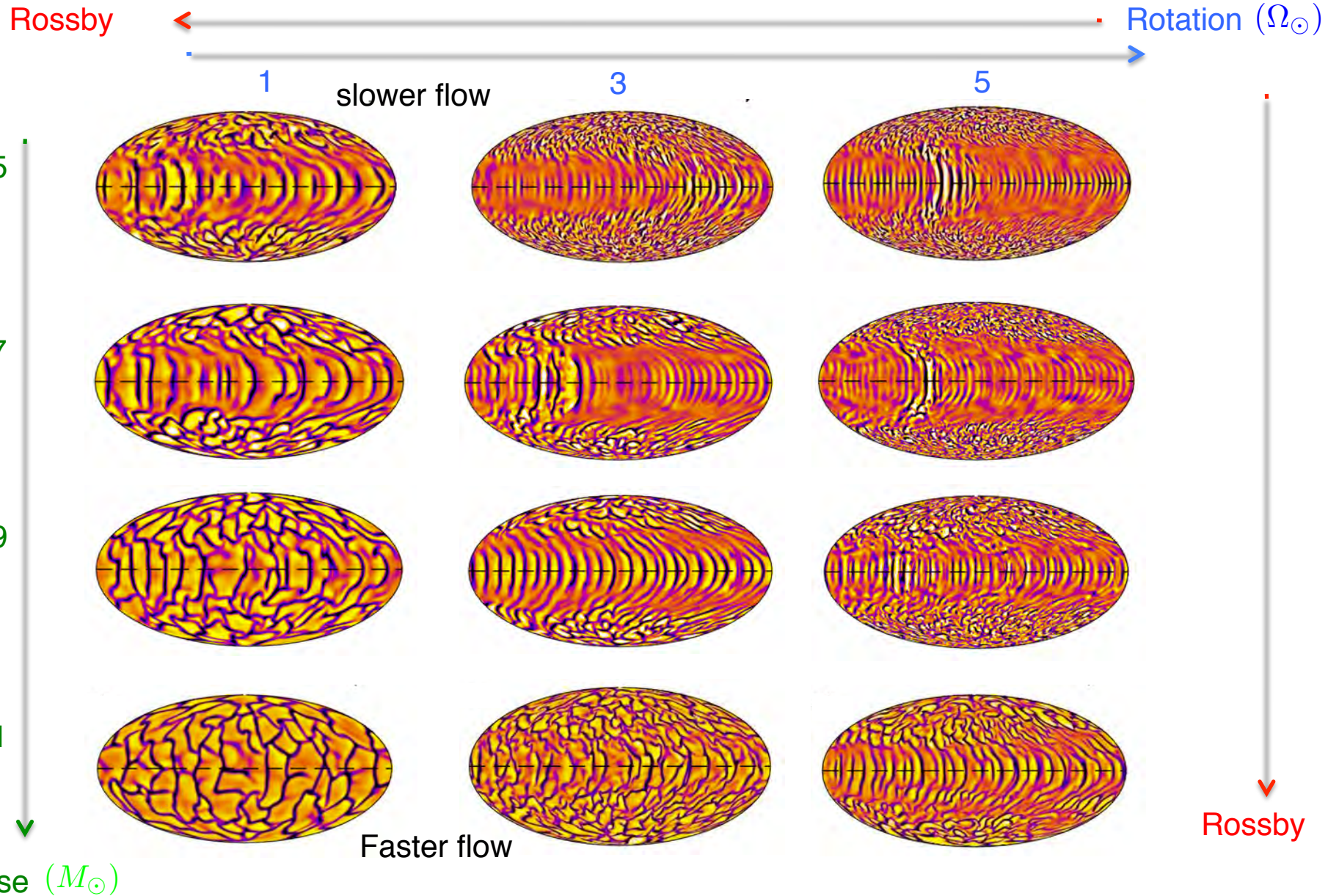
In Donahue et al. 1996: $\Delta\Omega \propto \Omega^{0.7}$

Collier-Cameron 2007

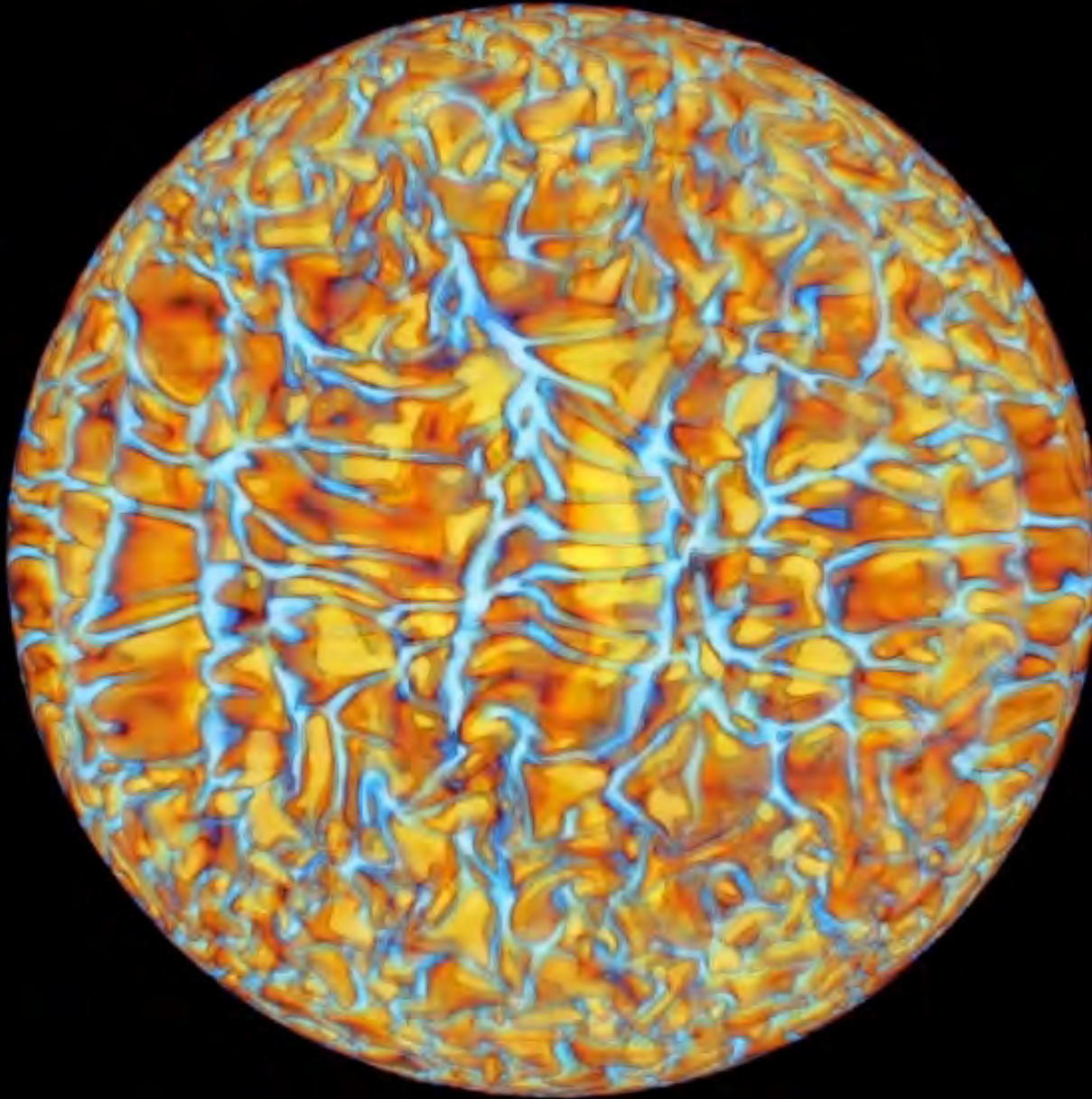
Confirming these observational scaling is key

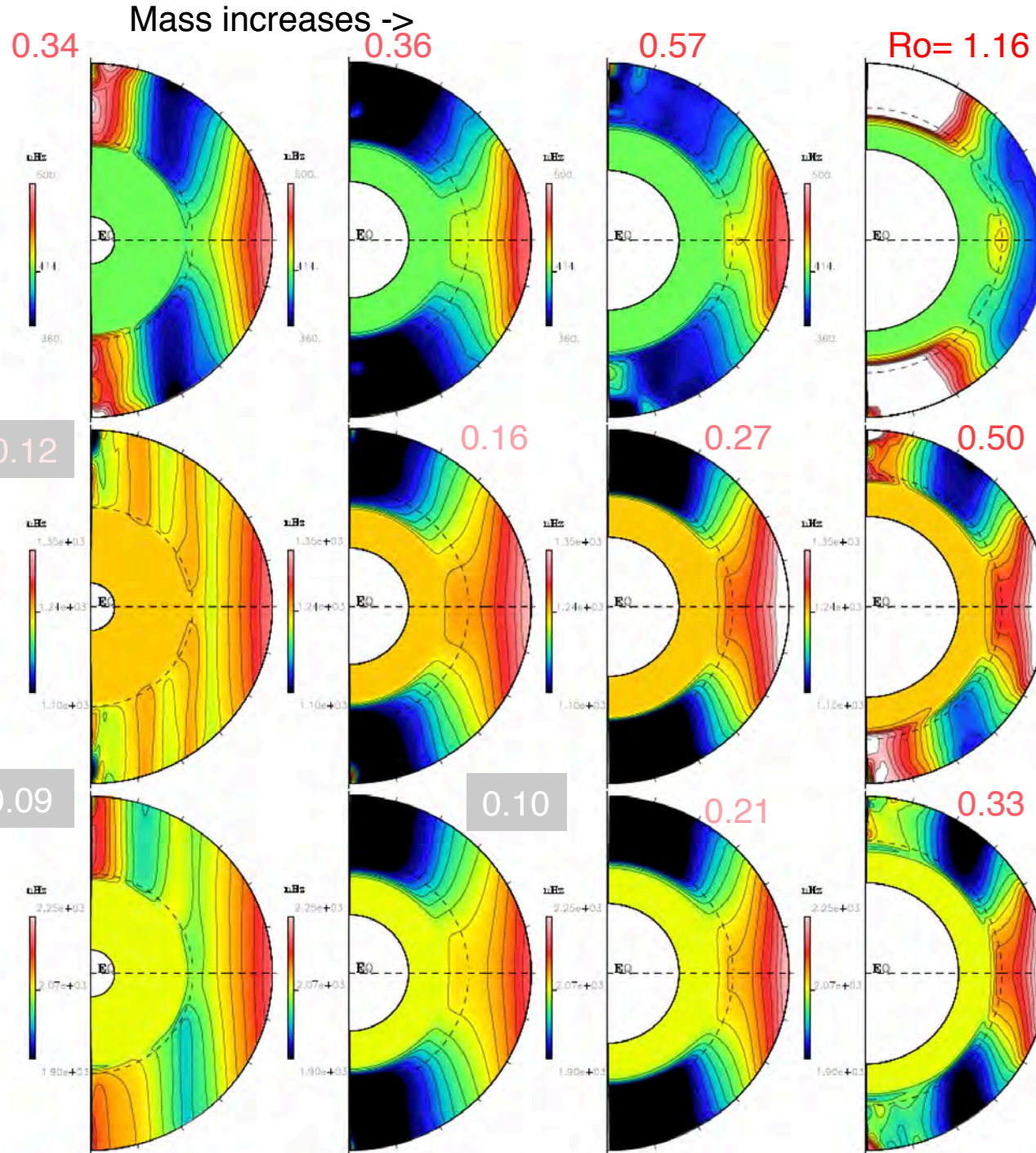
Effect of Rotation on Convection

Matt, DoCao, Brun et al. 2011, 2013



Turbulent Convection in Stars





Differential Rotation In G & K stars

Ω Matt et al. 2011
Brun et al. 2014

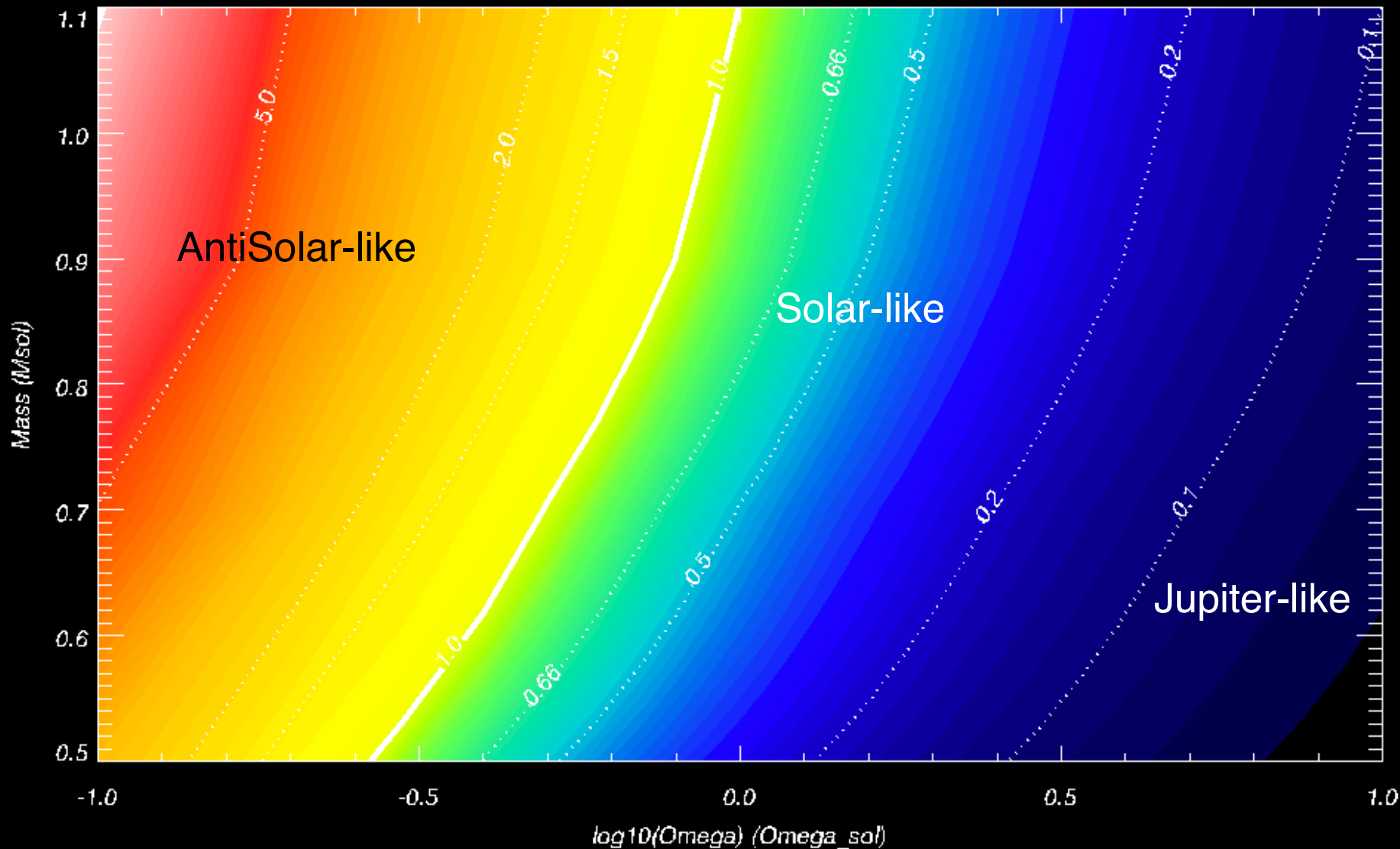
Rossby nb
 $Ro=\omega/2\Omega_*$

5 Ω

See also: Gastine et al. 2014
Kapyla et al. 2013

Rossby Number vs Stellar Mass and Rotation

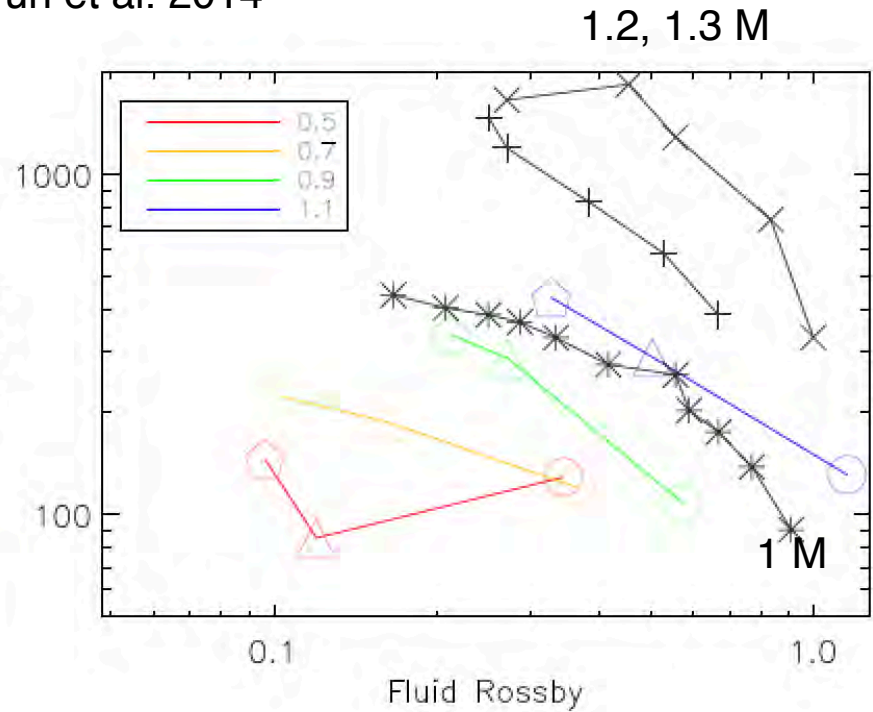
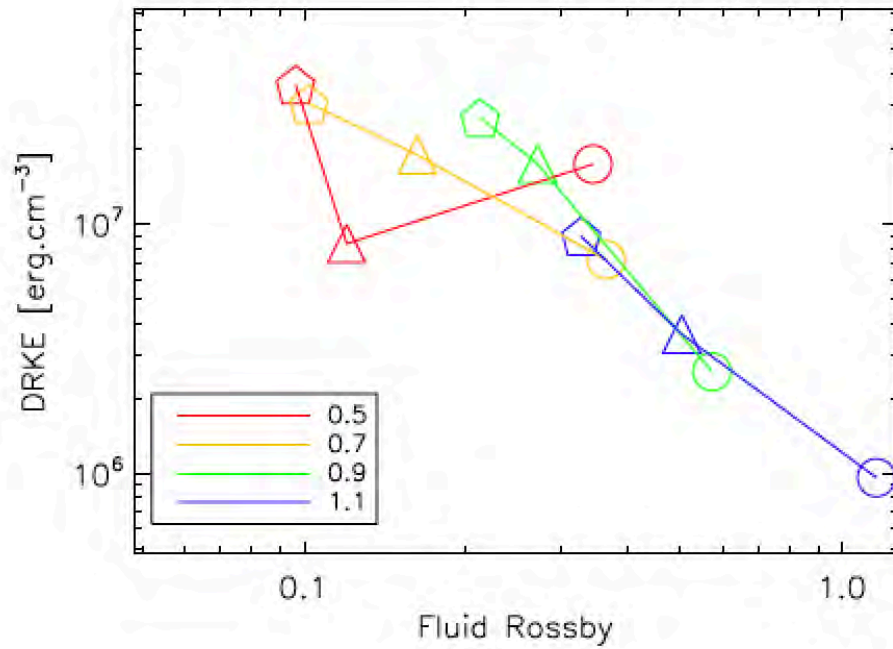
Rossby Nb: Solar vs Anti-solar Diff Rot - A.S.Brun (CEA-Saclay)



Brun et al. 2014, 2015

Scaling Law for $\Delta\Omega$

Matt et al. 2011, Brun et al. 2014



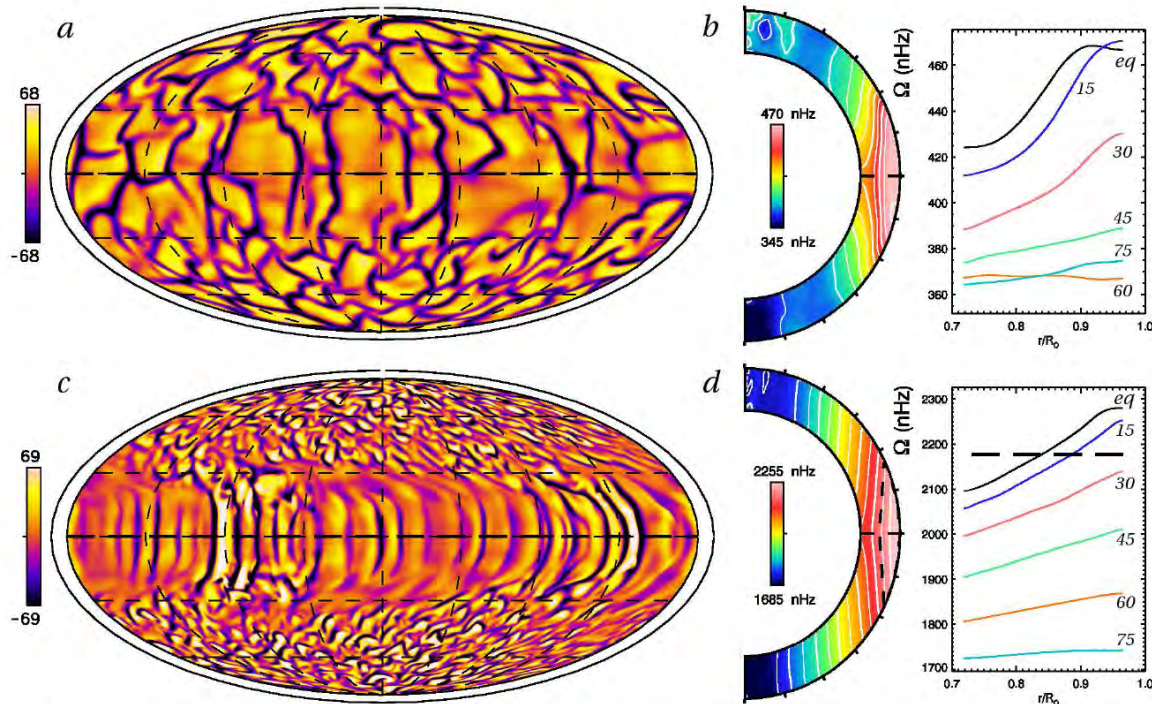
Brown et al. 2008
Augustson et al. 2012

$$\Delta\Omega = 156.0 \text{ nHz} \left(\frac{M}{M_{\odot}} \right)^{1.0} \left(\frac{\Omega_0}{\Omega_{\odot}} \right)^{0.47}$$

$$= 150.3 \text{ nHz} \left(\frac{M}{M_{\odot}} \right)^{1.85} R_{\text{of}}^{-0.52}$$

Smaller $\Delta\Omega$ with smaller Mass

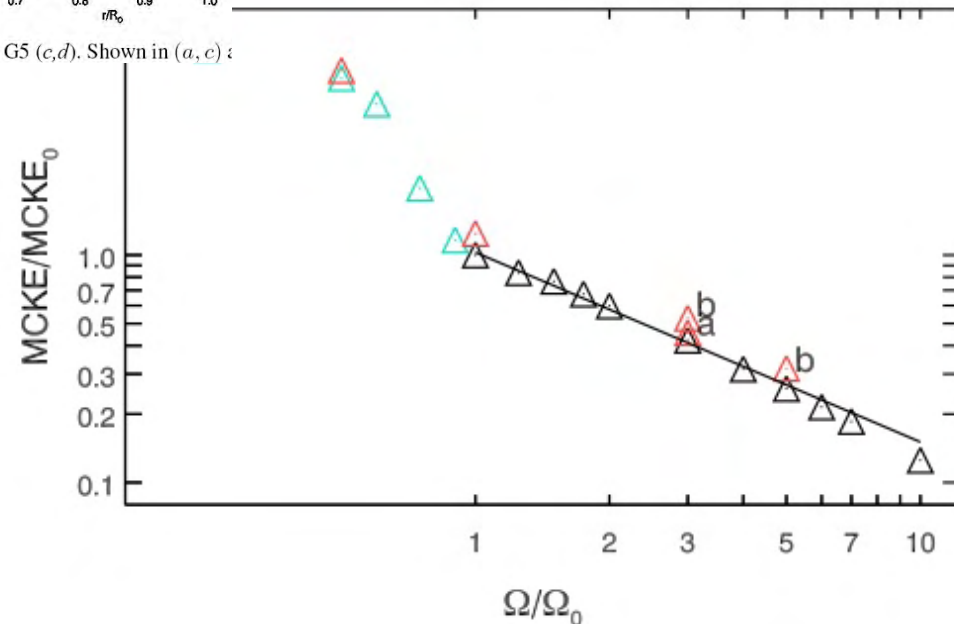
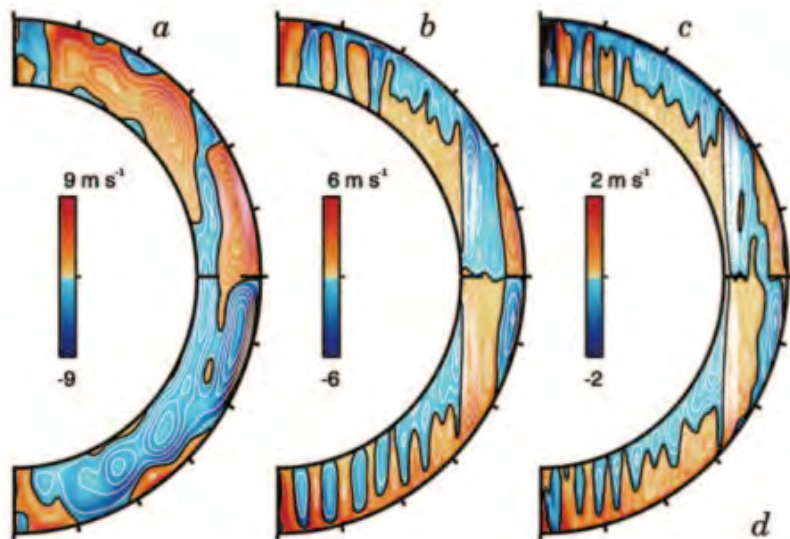
Guessing a scaling with rotation of meridional flows



Dikpati et al. 2001 assumed $V_p \sim \Omega$
 Charbonneau & Saar 2001 assumed $V_p \sim \Omega$ or $\log(\Omega)$

Scaling of MC deduced from Brown et al. 2008

Fig. 1 Evolution of global-scale convective flows with increasing rotation rate for case G1 (a,b) and case G5 (c,d). Shown in (a, c) :



Stellar Magnetism: observations and models

Solar Type Stars (late F, G and early K-type)

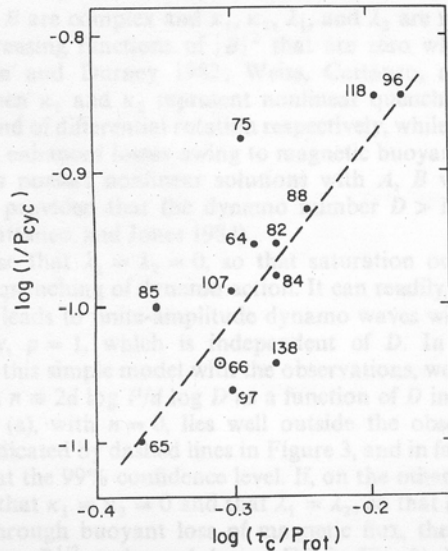


FIG. 2.— $\log(1/P_{cyc})$ vs. $\log(\tau_c/P_{rot})$ for the stars of Table 1. The dashed line is a linear least squares fit to the data.

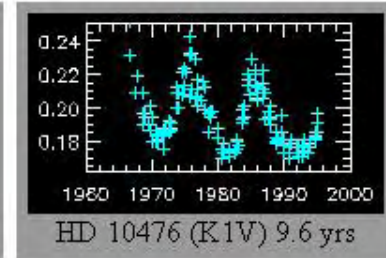
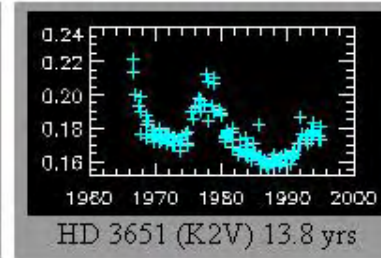
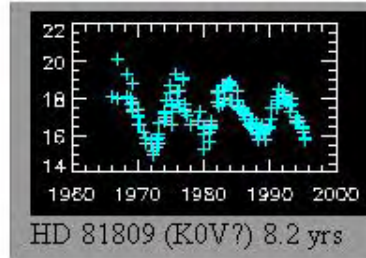
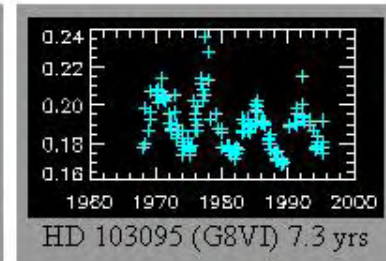
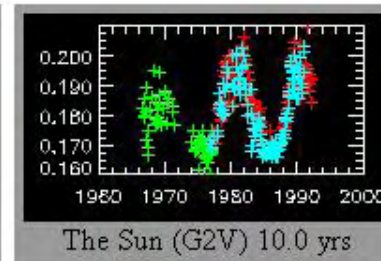
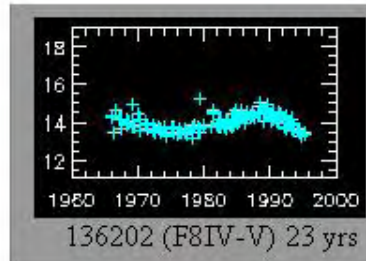
Noyes et al. 1984

In stars activity depends on rotation
& convective overturning time
via Rossby nb $Ro = P_{rot}/\tau$

$$\langle R'_{HK} \rangle = Ro^{-1}, \quad P_{cyc} = P_{rot}^{1.25 \pm 0.5}$$

Wilson 1978

Baliunas et al. 1995



Call H & K lines, $\langle R'_{HK} \rangle$

Over 111 stars in HK project (F2-M2):

31 flat or linear signal

29 irregular variables

51 + Sun possess magnetic cycle

=>

Much more
coming in
Asteroseismology
Era (Mike's talk)

Quid of Star-Planet Interaction and cyclic activity?

Magnetic cycles of the planet-hosting star τ Bootis

J.-F. Donati,^{1★} C. Moutou,^{2★} R. Farès,^{1★} D. Bohlender,^{3★} C. Catala,^{4★} M. Deleuil,^{2★}
E. Shkolnik,^{5★} A. C. Cameron,^{6★} M. M. Jardine^{6★} and G. A. H. Walker^{7★}

Solar Analogs

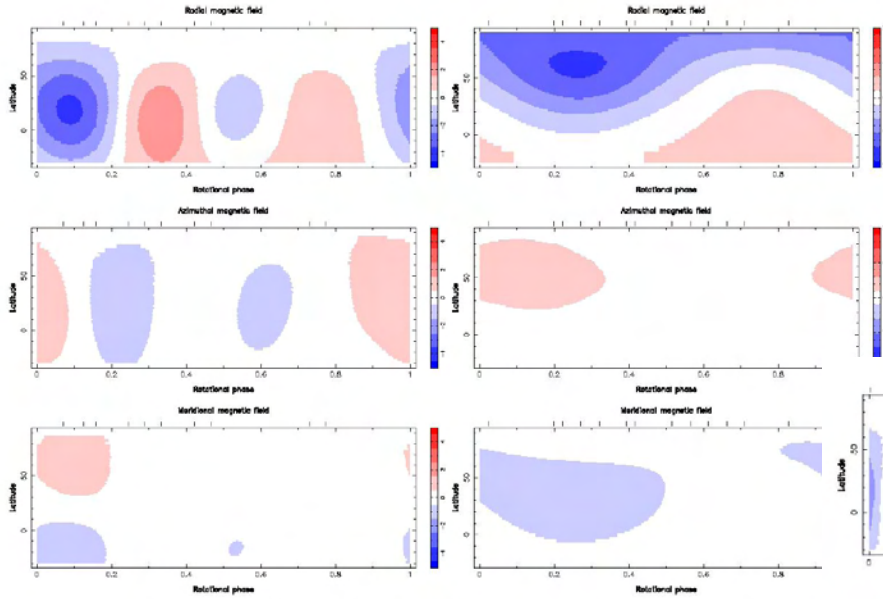


Figure 4. Magnetic maps of HD 146233 and HD 76151 (left and right panel, respectively). Each chart illustrates the onto one axis of the spherical coordinate frame. The magnetic field strength is expressed in Gauss. Vertical ticks above the observed rotational phases. Note that color scales are not the same for every star.

Faster the solar analogs rotate more toroidal Field contribution they possess.

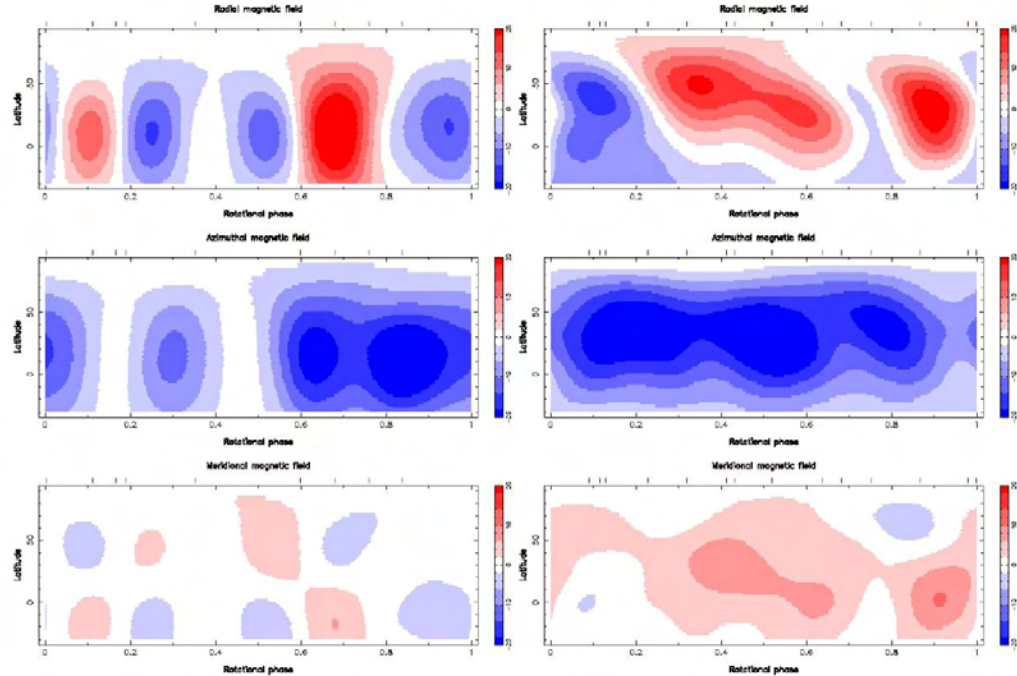


Figure 5. Same as Fig. 4, for HD 73350 (left panel) and HD 190771 (right panel).

Stellar Magnetism vs Stellar Dynamo

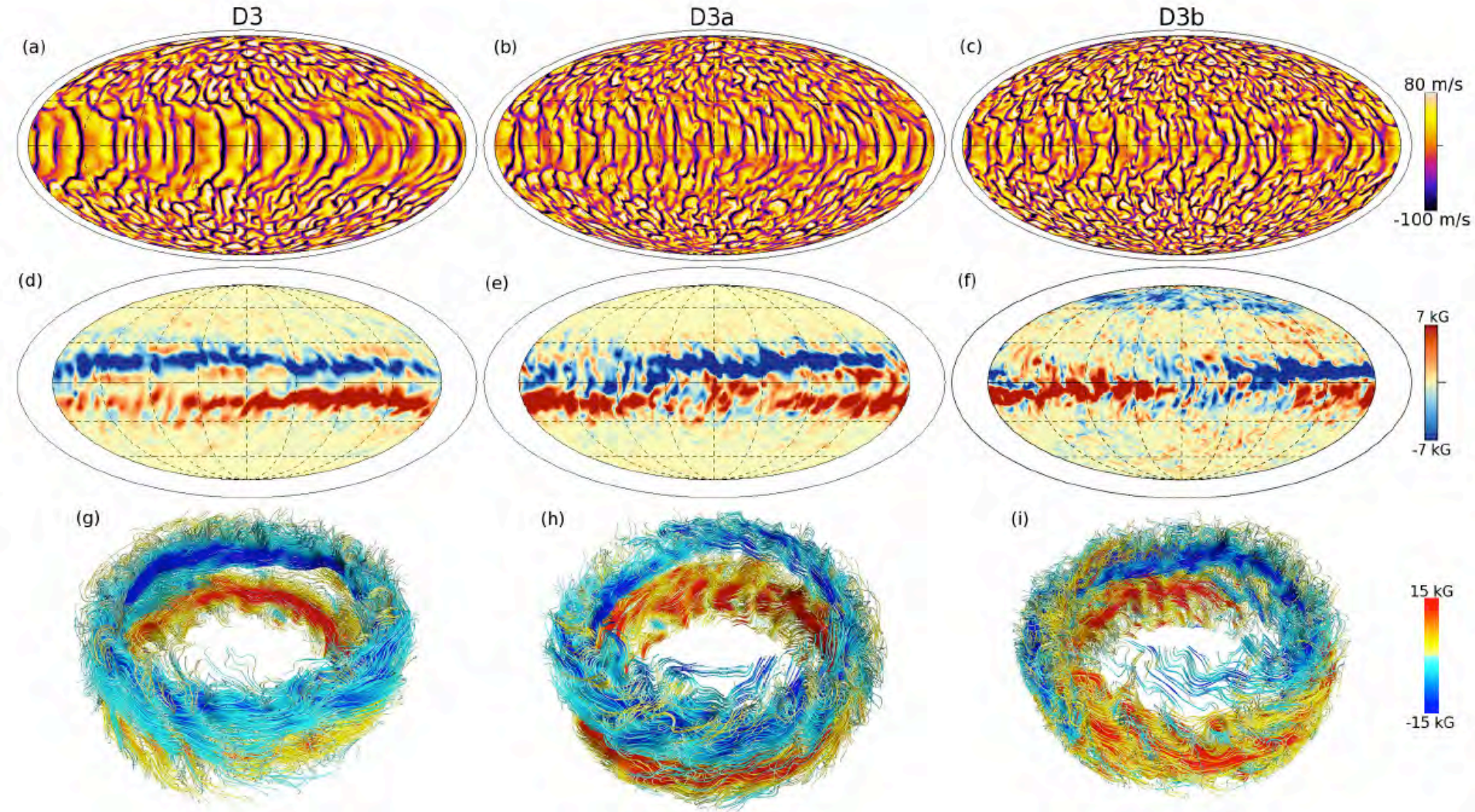
- Source of variability (chaos, intermittency,...)
- Existence of **starspot** and sensitivity to stellar parameters
- Can we reproduce the trend $P_{\text{cyc}} \sim P_{\text{rot}}^n$ (with $n \sim 1 \pm 0.2$)
- Can we reproduce the rise of the toroidal vs poloidal field
- What can we do about MC flow profile and amplitude?
- Which « solar model » is best to explain stellar data?

BL mean field
models

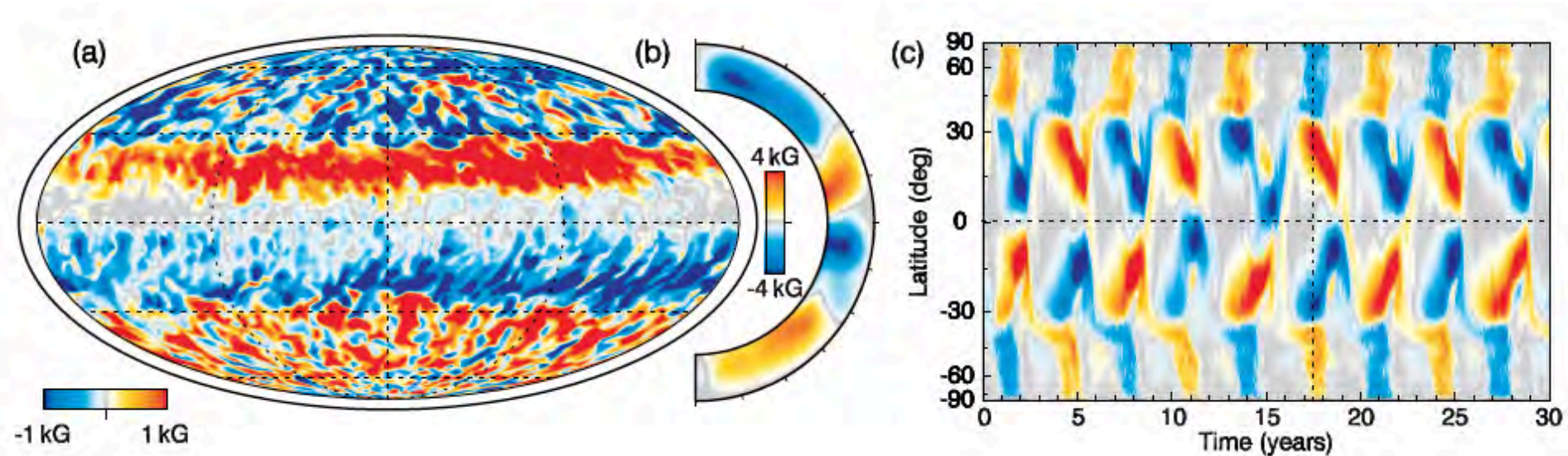
$$P_{\text{cyc}} = v_0^{-0.91} s_0^{-0.013} \eta^{-0.075} \Omega_0^{-0.014}$$

Strong dependancy on meridional flow amplitude

Magnetic Wreaths vs Turbulence



Latest solar-like case D3: getting cycle and equatorward branch



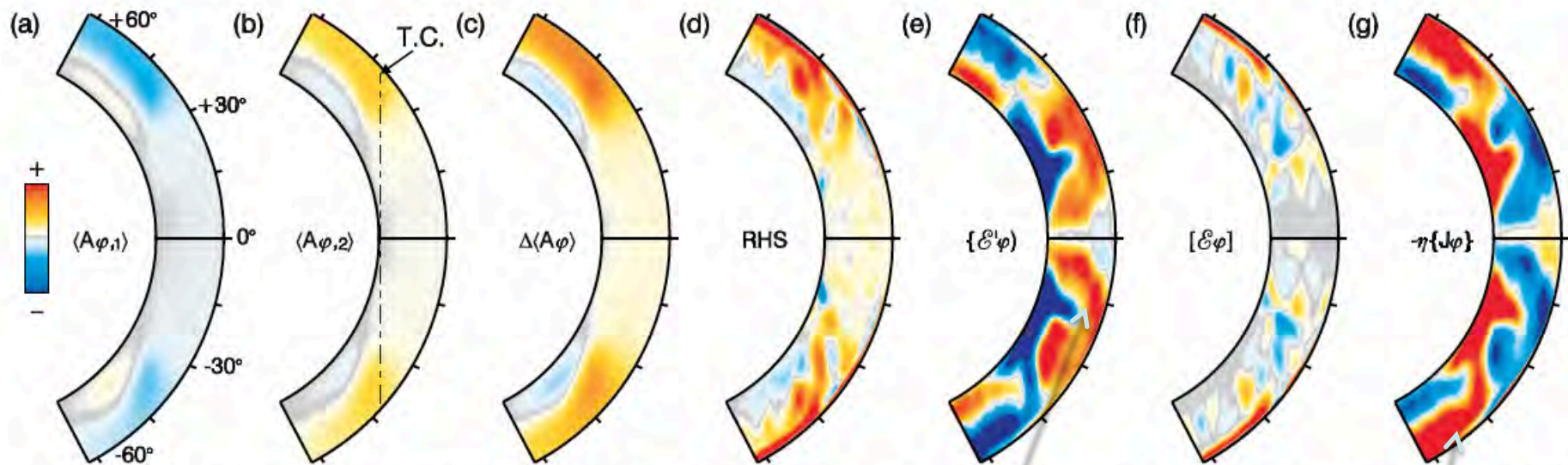
Reducing ν even further ν by using SLD scheme makes the simulation develop a more regular cyclic behavior

Augustson, Brun et al. 2013, ApJL, submitted

Origin of Poloidal Field Reversal

$$\Delta \langle A_\varphi \rangle = \langle A_{\varphi,2} \rangle - \langle A_{\varphi,1} \rangle = \{ \mathcal{E}'_\varphi \} + [\mathcal{E}_\varphi] + \eta \{ J_\varphi \}$$

$$= \int_{t_1}^{t_2} dt \hat{\varphi} \cdot \langle \mathbf{v}' \times \mathbf{B}' \rangle + \int_{t_1}^{t_2} dt \hat{\varphi} \cdot (\langle \mathbf{v} \rangle \times \langle \mathbf{B} \rangle) - \int_{t_1}^{t_2} dt \eta \langle J_\varphi \rangle.$$



Fluctuating Emf key term

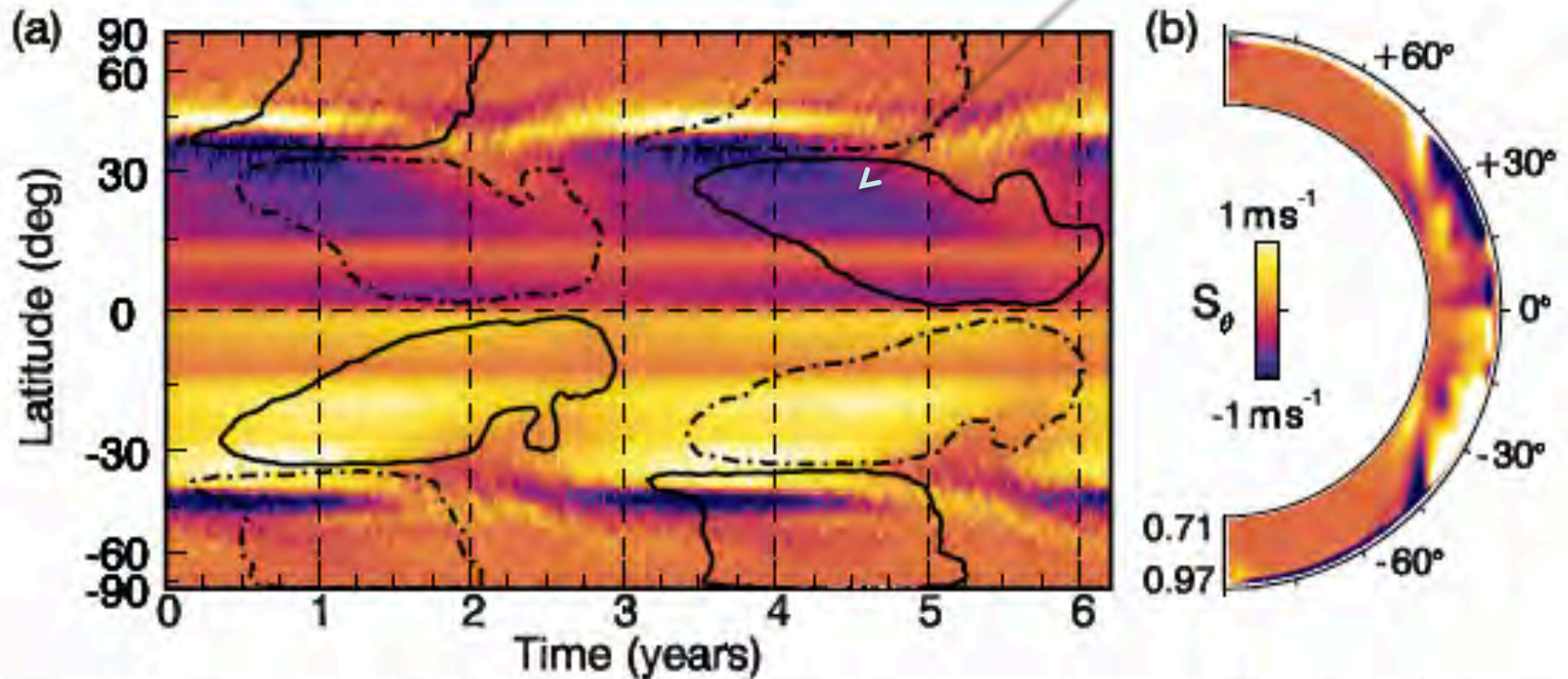
some contribution
from diffusion term
at high latitudes

In kinematic theory the propagation direction of such a wave is given by the Parker-Yoshimura rule (e.g., Parker 1955; Yoshimura 1975) as

$$\mathbf{S} = -\lambda \bar{\alpha} \hat{\phi} \times \nabla \frac{\Omega}{\Omega_0}, \quad (19)$$

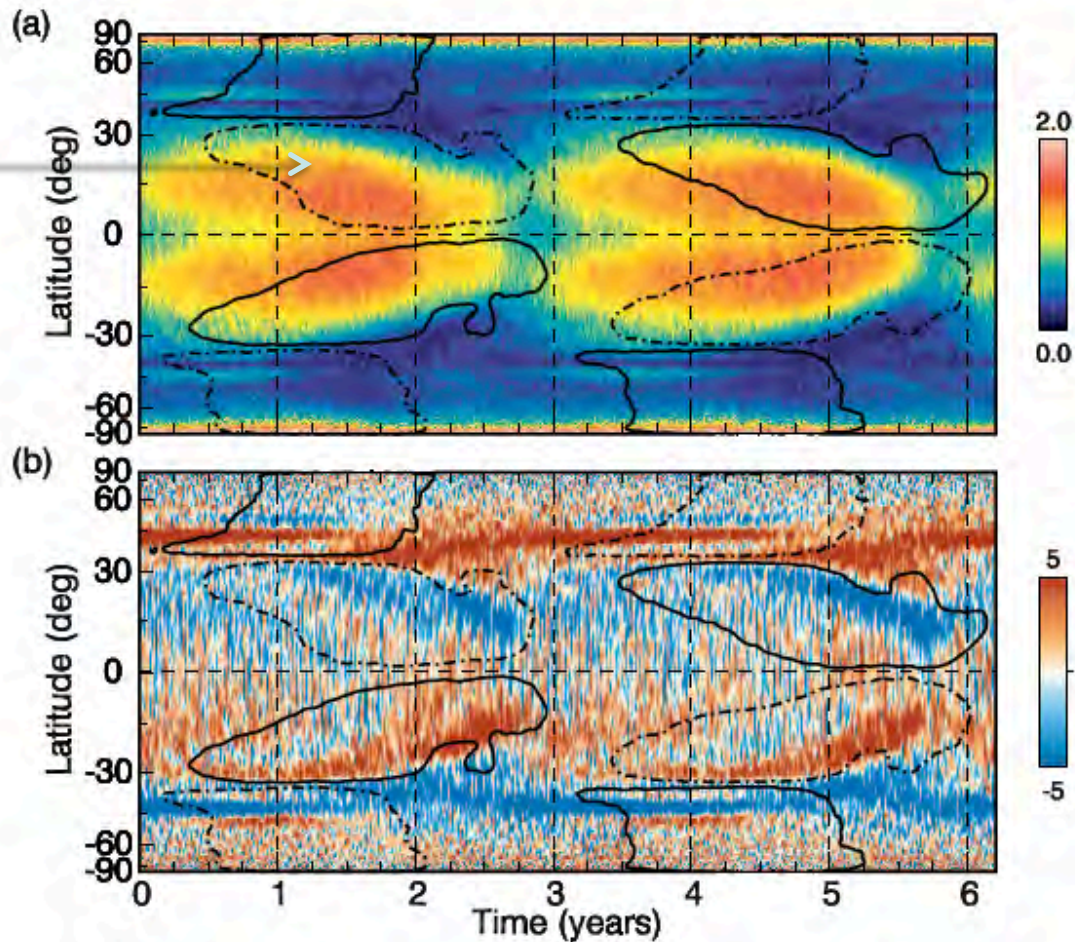
where $\lambda = r \sin \theta$ and $\bar{\alpha} = -\tau_o \langle \mathbf{v}' \cdot \boldsymbol{\omega}' \rangle / 3$. Thus $\bar{\alpha}$ depends on the convective overturning time τ_o and the kinetic helicity.

Parker-Yoshimura Rule



Non-linear dynamo wave

Correct sign

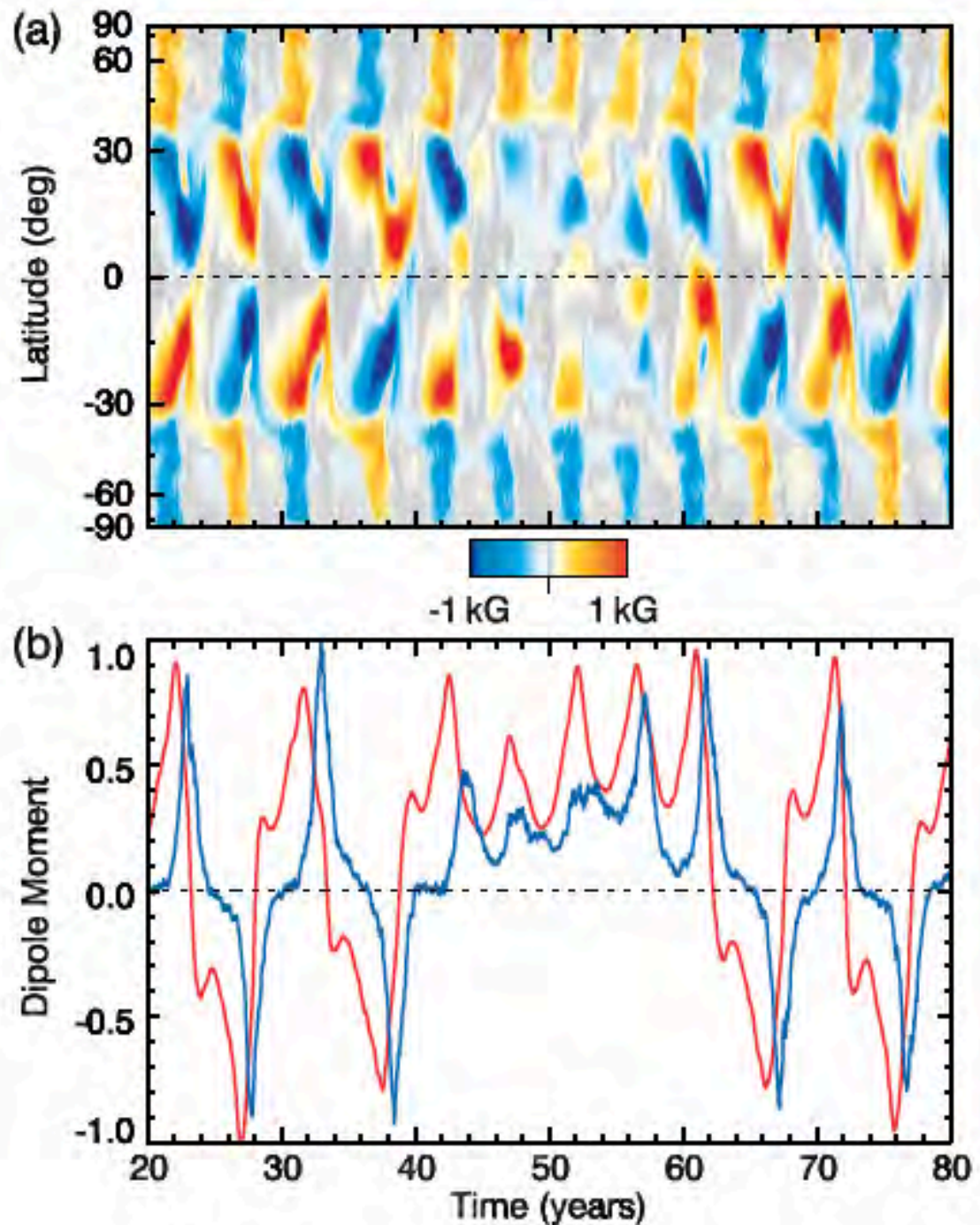


Interaction between
Shear and B_φ

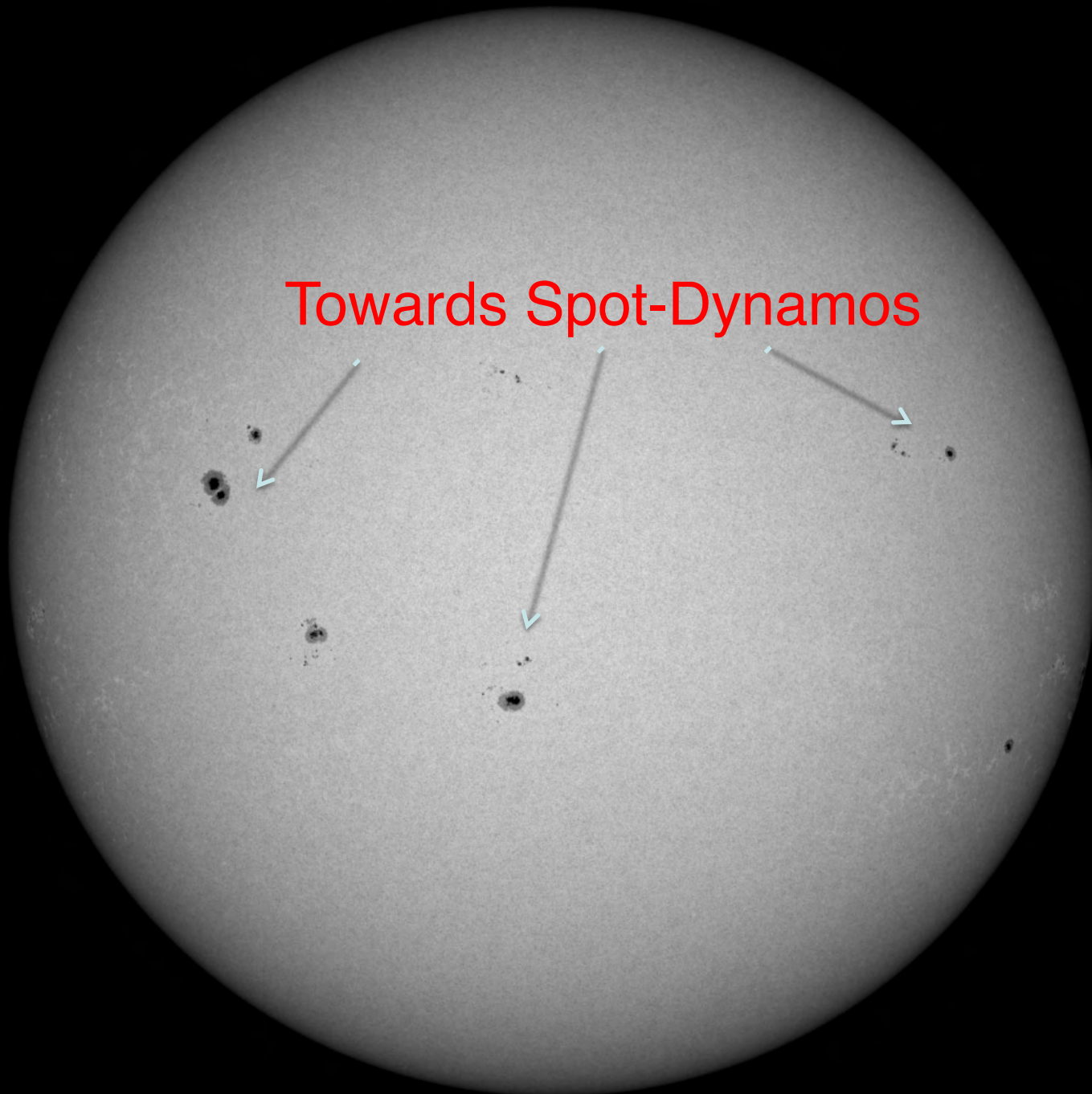
Figure 11. Coevolution of the mean toroidal magnetic field $\langle B_\varphi \rangle$ at $0.92R_\odot$ over the average magnetic polarity cycle with (a) the magnitude of the mean angular velocity gradient $R_\odot |\nabla \Omega| / \Omega_0$ and (b) latitudinal velocity $\langle v_\theta \rangle$ of the evolving meridional circulation in units of m s^{-1} . Here $\langle B_\varphi \rangle$ is overlain with positive magnetic field as solid lines and negative field as dashed lines, with the contours corresponding to a 1 kG strength field.

Latest solar-like case DS3:
Getting Maunder like minimum

Quadrupole dominates over
Dipole during reversal and
Grand minimum phase



Towards Spot-Dynamos



Magnetic Wreath and Intermittency yielding flux emergence

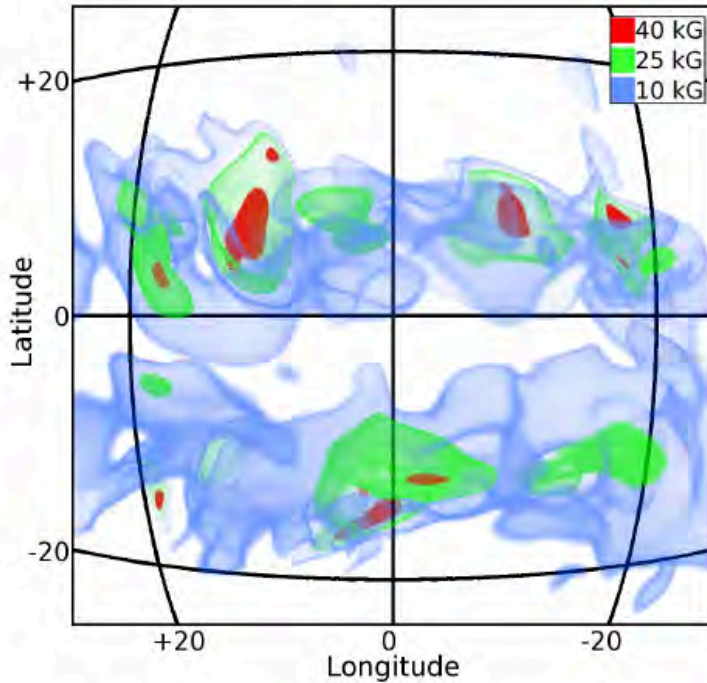


Figure 17. Three-dimensional volume renderings of isosurfaces of magnetic field amplitude in case S3. Blue surfaces have amplitudes of 10 kG, green surfaces represent 25 kG, and red surfaces indicate 40 kG fields. Grid lines indicate latitude and longitude at $0.72 R_{\odot}$ as they would appear from the vantage point of the viewer. Small portions of the cores of these wreaths have been amplified to field strengths in excess of 40 kG while the majority of the wreaths exhibit fields of about 10 kG or roughly in equipartition with the mean kinetic energy density (see Figure 2).

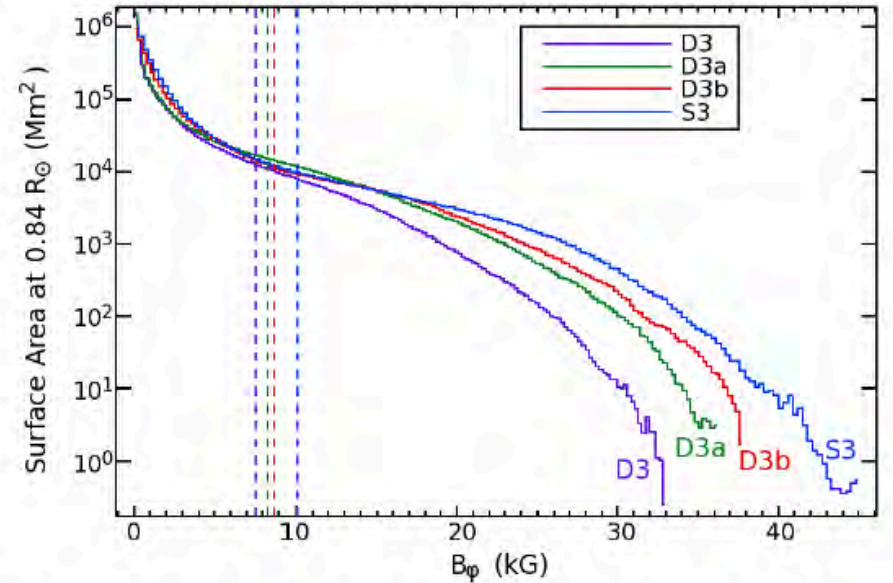
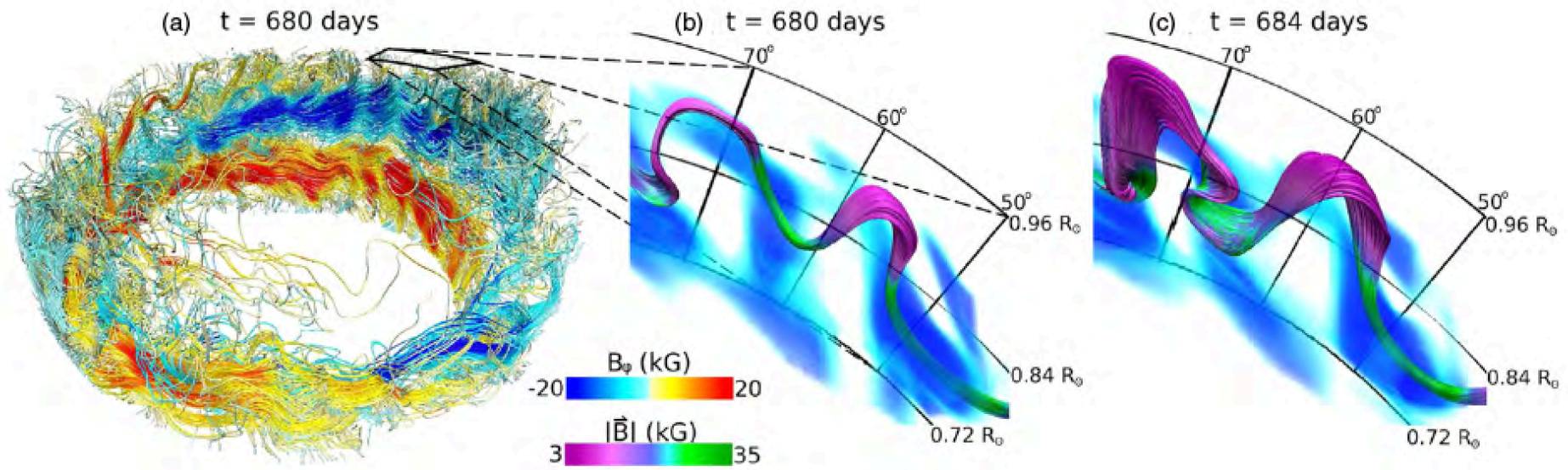


Figure 2. Probability distribution functions for unsigned B_{ϕ} at mid-convection zone for cases D3 (purple), D3a (green), D3b (red), and S3 (blue) showing the surface area covered by fields of a given magnitude. Distributions are averaged over about 300 days when fields are strong and as steady as possible. Dashed vertical lines show the field-strength at which equipartition is achieved with the maximum fluctuating kinetic energy (FKE) at mid-convection zone for each case. Case D3b shows a deficit of field in the 10 kG range, but an excess of surface area covered by extremely strong fields above 25 kG range, as well as higher peak field strengths. Case S3 shows significantly greater regions of fields in excess of 20 kG than all other cases.

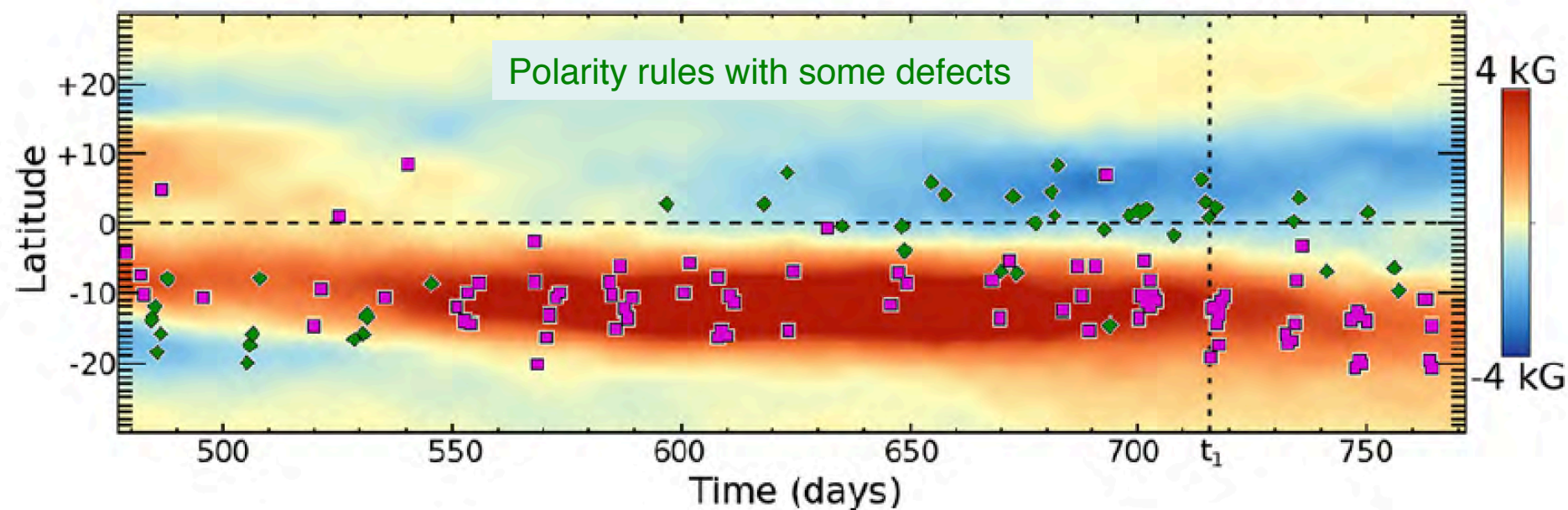
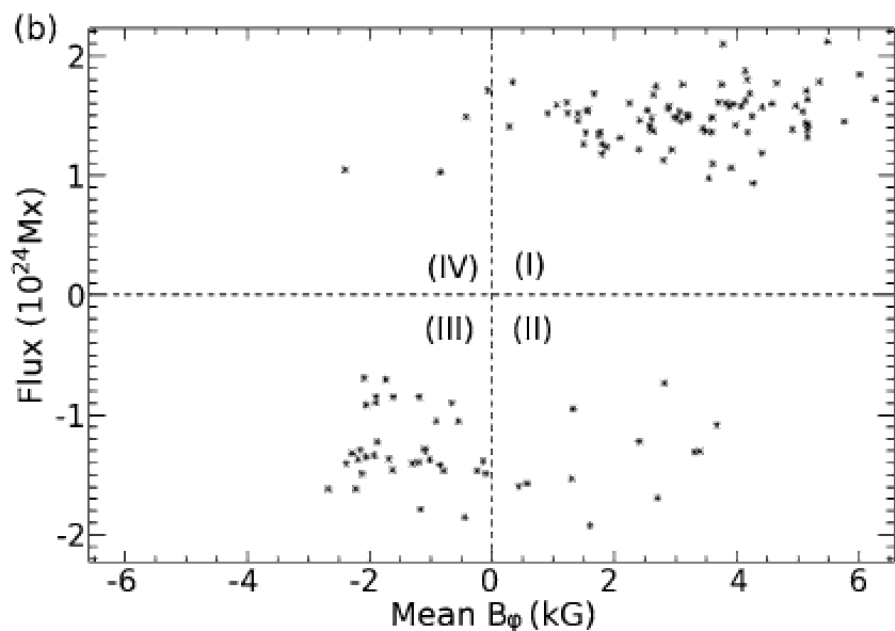
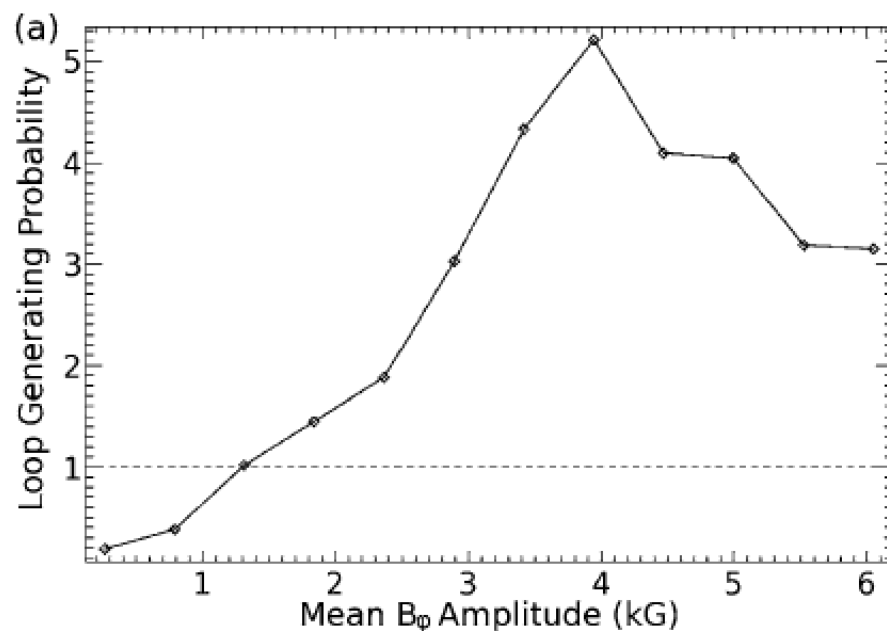
Wreaths can generate Buoyant Loops



Nelson et al. 2011, 2013a, 2013b

□ Towards getting first “spot-dynamos”...

Statistic of Buoyant Loops



Conclusions

Convective velocities V_r roughly scales with **cubic root** of $L_*/(R_*^2 \rho_{\text{meanCZ}})$ (star's luminosity divided by mean density in CZ)

⇒ **Prograde** vs **retrograde** state changes at different Ω_0 as spectral type is changed (since $Ro = V/2\Omega_0 L$ and V changes with spectral type)

⇒ **Cylindrical** vs **conical** vs **shellular** differential profiles depends on **Reynolds** stresses & **thermal** (baroclinic) effects/**tachocline**

⇒ **Magnetic field** B reduces or can even suppress diff rot Ω

⇒ at **high** rotation rate we get **magnetic wreaths** that generate **omega-loops** as we lower diffusivity, **cyclic dynamos** easier to get

⇒ Multipolar or Dipolar magnetic **bi-stability** exist but Multipolar fields seem to dominate at **high stratification**

⇒ Stratification and/or a tachocline may help getting **equatorward** butterfly diagram (shift location of Ω and α -like effects)

